Preprint of the paper:
Blocken B, Carmeliet J. 2004. A review of wind-driven rain research in building science. Journal of Wind Engineering and Industrial Aerodynamics 92(13): 1079-1130.

A review of wind-driven rain research in building science

Bert Blocken[•] [a], Jan Carmeliet [a,b]

(a) Laboratory of Building Physics, Department of Civil Engineering, Katholieke Universiteit Leuven, Kasteelpark Arenberg 51, 3001 Leuven, Belgium
(b) Building Physics Group, Faculty of Building and Architecture, Technical University Eindhoven, P.O. Box 513, 5600 MB Eindhoven, The Netherlands

Abstract

Wind-driven rain or driving rain is rain that is given a horizontal velocity component by the wind. Wind-driven rain research is of importance in a number of research areas including earth sciences, meteorology and building science. Research methods and results are exchangeable between these domains but no exchanges could yet be noted. This paper presents the state-of-the-art of wind-driven rain research in building science. Wind-driven rain is the most important moisture source affecting the performance of building facades. Hygrothermal and durability analysis of facades requires the quantification of the wind-driven rain loads. Research efforts can be classified according to the quantification methods used. Three categories are distinguished: (1) experimental methods, (2) semi-empirical methods and (3) numerical methods. The principles of each method are described and the state-of-the-art is outlined. It has been the intent of the present paper to bring together the reports, papers and books - published and unpublished - dealing with wind-driven rain research in building science to provide a database of information for researchers interested in and/or working in wind-driven rain research, independent of their field of expertise.

Keywords: Wind; Rain; Wind-driven rain; Driving rain; Building; CFD; Quantification

1. Introduction

Wind-driven rain (WDR) or driving rain is rain that is given a horizontal velocity component by the wind and that falls obliquely. WDR research is important in a number of research areas including earth sciences, meteorology and building science.

WDR over unlevel ground such as hills or valleys results in a redistribution of raindrops by local wind flow deformations that can cause large precipitation variations [1-12]. Knowledge of the distribution of WDR on hills and in valleys is important for catchment hydrology [4, 13], for the design of rainfall monitoring networks [14], runoff and erosion studies [7, 8], determination of cropping conditions and studies of the topographic distribution of forest-fire danger [15]. WDR conditions also determine the representativeness of point rain measurements on hill slopes [3, 15-20], near buildings [21] and near trees or other obstructions [22]. Furthermore, WDR is responsible for errors in precipitation measurements by individual above-ground gauges. Due to the deflection of the wind flow and raindrop trajectories by the gauge body the gauge does not catch a representative sample of the rain reaching the earth's surface [23-33]. The inclusion of WDR research in erosion studies is imperative as the obliqueness and increased kinetic energy of rainfall influence processes such as soil detachment and can cause raindrop splash anisotropy and upslope splash drift [7, 34-52]. WDR can also play an important role in the canopy tree interception of rain [53], in rainfall interception by plants (comments by Fourcade [17] on Phillips [54, 55]) and in spore removal and spreading of plant diseases [56, 57].

WDR is also an important research subject in building science. It is the most important moisture source affecting the hygrothermal performance and durability of building facades (Eldridge [58], Lacasse and Vanier [59, 60]). Consequences of its destructive properties can take many forms. Moisture accumulation in porous materials can lead to water penetration [58, 61-72], frost damage [58, 73-76], moisture induced salt migration [73, 76, 77], discoloration by efflorescence [58, 76], structural cracking due to thermal and moisture gradients [76], to mention just a few. WDR impact and runoff is also responsible for the appearance of surface soiling

[•] Corresponding author: Bert Blocken, Laboratory of Building Physics, K.U.Leuven, Kasteelpark Arenberg 51, 3001 Leuven, Belgium. Tel.: +32 (0) 16-321345 - Fax: +32(0) 16-321980
E-mail address: bert.blocken@bwk.kuleuven.ac.be

patterns on facades that have become characteristic for so many of our buildings [58, 78-90]. Although these issues have been widely and for a long time recognized as major building problems, damage claims and huge repair and replacement costs are still on the rise [91, 92]. Two reasons are feeding the persistence of these problems. First, there is the increasing use of innovative design features, building technologies and materials in present-day construction, knowledge on the hygrothermal performance of which has not yet been fully attained. Second, unlike most requirements of buildings where the design data can be expressed in quantitative terms, appropriate quantitative design data for WDR are lacking.

The study of WDR in building science consists of two parts, namely (1) the quantification of WDR loads and (2) the study of the response of the building to these loads. In the context of this paper only the former will be addressed. Issues beyond the scope of the paper are cloud and raindrop physics, surface phenomena such as splashing, runoff, evaporation and absorption, mechanisms of rain penetration in buildings and the development and execution of watertightness tests. The quantity of WDR impinging on building facades is governed by a diversity of parameters: building geometry, environment topology, position on the building facade, wind speed, wind direction, turbulence intensity, rainfall intensity, raindrop size distribution and rain event duration. The large number of parameters and their variability make the quantification of WDR a highly complex problem. It is not surprising that despite research efforts spanning over almost a century, WDR is still an active research subject in building science and a lot of work remains to be done. A particularly large number of research efforts have already been devoted to examining the exposure of building facades to WDR. It is the intent of the present paper to bring together the reports, papers and books - published and unpublished - dealing with the quantification of WDR on buildings and to provide a database of information for researchers interested in and/or working in WDR research, independent of their field of expertise. To the knowledge of the authors, no complete literature review on WDR research currently exists. In a first part of the paper, definitions and parameters are given. Next, the review is split up into three parts according to the methods for quantifying WDR: (1) experimental methods, (2) semi-empirical methods and (3) numerical methods.

2. Wind-driven rain and buildings – Definitions and parameters

The joint occurrence of wind and rain causes an oblique rain intensity vector. In building science, oblique rain is referred to as either “driving rain” or “wind-driven rain”, whereas in earth sciences and meteorology, the latter term is practically always used. This term will also be used in the present paper (WDR). In general, “WDR intensity” refers to the oblique rain vector. From the viewpoint of the interaction between rain and vertical building facades, the term "WDR intensity" however takes on the narrower meaning of “component of the rain intensity vector causing rain flux through a vertical plane”. The latter definition was adopted by the CIB (International Council for Building Research) [93] and is used in the present paper (Fig. 1). The other component of the rain intensity vector, that causes rain flux through a horizontal plane, is termed (horizontal) rainfall intensity.

When wind approaches a building, a disturbance is generated and a specific flow pattern develops around it, including a frontal vortex, separation at building corners, corner streams, recirculation zones, shear layers and a far wake [94]. When rain is added to the flow field, it will be driven against the windward facade of the building (Fig. 2). As a result of the specific flow features, the course of the raindrop trajectories is changed which results in a non-uniform wetting of the facade.

Several quantities have been defined for describing the WDR load on facades. In the present paper, we will use the specific catch ratio η_d, related to the raindrop diameter d, and the catch ratio η, related to the entire spectrum of raindrop diameters (Eq. (1)).

$$\eta_d(d,t) = \frac{R_{wdr}(d,t)}{R_h(d,t)}, \quad \eta(t) = \frac{R_{wdr}(t)}{R_h(t)} \tag{1}$$

$R_{wdr}(d,t)$ and $R_h(d,t)$ are the specific WDR intensity and specific unobstructed horizontal rainfall intensity for raindrops with diameter d. $R_{wdr}(t)$ and $R_h(t)$ respectively refer to the same quantities but integrated over all raindrop diameters. The unobstructed horizontal rainfall intensity is the intensity of rainfall through a horizontal plane that is situated outside the wind flow pattern that is disturbed by the building. In practical applications the (specific) catch ratio will be measured and calculated for discrete time steps $[t_j, t_j+\Delta t]$. The (specific) catch ratio for a discrete time step is redefined as:

$$\eta_d(d,t_j) = \frac{\int_{t_j}^{t_j+\Delta t} R_{wdr}(d,t)\,dt}{\int_{t_j}^{t_j+\Delta t} R_h(d,t)\,dt} = \frac{S_{wdr}(d,t_j)}{S_h(d,t_j)}, \quad \eta(t_j) = \frac{\int_{t_j}^{t_j+\Delta t} R_{wdr}(t)\,dt}{\int_{t_j}^{t_j+\Delta t} R_h(t)\,dt} = \frac{S_{wdr}(t_j)}{S_h(t_j)} \tag{2}$$

where $S_{wdr}(d,t_j)$ and $S_h(d,t_j)$ are the specific WDR amount (sum) and specific unobstructed horizontal rainfall amount (sum) during time step $[t_j, t_j+\Delta t]$ for raindrops with diameter d. $S_{wdr}(t_j)$ and $S_h(t_j)$ respectively refer to the same quantities integrated over all raindrop diameters. The WDR amount S_{wdr} for each time step is obtained by multiplying the catch ratio η with the unobstructed horizontal rainfall amount S_h for this time step. The catch ratio is a complicated function of space and time. The six basic influencing parameters for the catch ratio as defined in Eq. (1) are: (1) building geometry (including environment topology), (2) position on the building facade, (3) wind speed, (4) wind direction, (5) (horizontal) rainfall intensity and (6) (horizontal) raindrop size distribution. In reality, the turbulent dispersion of raindrops is an additional parameter. It is often neglected as will be discussed later. The parameters wind speed (m/s) and wind direction (degrees from north) are usually given as their values at 10 m height in the undisturbed flow (U_{10}, φ_{10}). The parameters horizontal rainfall intensity R_h (mm/h or L/m²h) and horizontal raindrop size distribution $f_h(d)$ (m^{-1}) refer to the rainfall intensity and raindrop size distribution falling through a horizontal plane in the undisturbed flow field.

Other researchers have been using different names and/or definitions to express the quantity of WDR. Most researchers have used the definitions of specific catch ratio and catch ratio given above, albeit sometimes with different names [95-109]. Names that have frequently been used are "Local Effect Factor LEF" instead of "specific catch ratio η_d" and "Local Intensity Factor LIF" instead of "catch ratio η". These names have been introduced by Choi [95-99]. Sometimes the name "driving-rain ratio k" is used instead of "catch ratio η" [104-106]. Other definitions have been used by Brown [110], van Mook et al. [111] and by Straube and Burnett [112, 113]. These authors expressed the WDR load by the ratio of the WDR intensity to the free WDR intensity, i.e. the WDR intensity that would exist in the absence of the building. This ratio is given the name "catch ratio κ" (Brown [110] and van Mook et al. [111]) or "rain admittance function RAF" (Straube and Burnett [112, 113]). In the following, only the terms specific catch ratio and catch ratio and the respective symbols η_d and η will be used.

3. Experimental methods

3.1. Wind-driven rain gauges and measurements

The experimental methods consist of measuring WDR with WDR gauges. Similar to the well-known rainfall gauges that are equipped with a horizontal aperture to measure rainfall, WDR gauges are characterized by a vertical aperture to collect the amount of WDR (Fig. 3). Two types of measurements can be distinguished: (1) measurements of the free WDR (i.e. the WDR that is not influenced by the presence of buildings or other obstructions[1]) and (2) measurements of the WDR on buildings. Free WDR gauges are placed in “free field conditions” on a post to obtain a general idea of the WDR conditions, whereas wall-mounted WDR gauges are intended to obtain specific information of the WDR exposure at certain positions of the facade.

3.1.1. Free-standing wind-driven rain gauges

The earliest measurements of free WDR reported were made in 1816 as mentioned by Middleton [114]. The instrument concerned was invented by Kerr (Annals of Philosophy [115]). It was a vectopluviometer with a horizontal and a vertical opening that was always facing the wind by a vane. Other vectopluviometers were conceived by Knox (1837, [116]), Phillips (1840, [117]) and Chrimes (1872, [118]). The instrument of Knox had only the vertical collector and one set of eight compartments. The instruments of Phillips and Chrimes had no moving parts. They were an assembly of five rain gauges, one facing upward and the other four with vertical faces facing the cardinal directions. The intention of these instruments was to determine the average azimuth and inclination of rain and/or to determine the distribution of rain between various directions. These gauges were used in earth sciences and meteorology, not for building research.

The first free-standing WDR gauges used in building research were designed in 1936 by Beckett at the Building Research Station (BRS) in the UK [119, 120] and in 1937 by Holmgren at the Norwegian[2] Building Research Institute (NBRI) [121-125]. Both gauges are illustrated in Fig. 4. The BRS gauge (Fig. 4a) has eight vertical apertures for collecting WDR (8-way gauge), whereas its Norwegian counterpart (Fig. 4b) has four (4-

[1] In many cases the WDR gauges for measurement of the free WDR have been placed too close to buildings, trees and/or other obstructions. This will undoubtedly have influenced the WDR catches. Nevertheless we will indicate them with the term “free” WDR.

[2] It is not surprising that the cradle of WDR research is situated in Norway and the UK, countries with a long coastline in proportion to their land area. A large fraction of these countries suffers from a marked, oceanic climate with severe WDR exposure.

way gauge). The purpose of the free-standing gauges was twofold: (1) obtaining directional information from the catches of the apertures facing different directions and (2) obtaining free-standing WDR amounts as an indication of the amounts falling on building facades. For completeness, two special gauges designed at the Technical University of Denmark (TUD) are mentioned and illustrated in Fig. 5: a circular and a funnel-shaped free-standing WDR gauge (by Korsgaard and Madsen [126-129]). Furthermore, we mention the WDR measurement tower designed by Choi [130-132], which resembles the Norwegian 4-way gauge but with an important additional feature, which will be explained later.

An important part of WDR research in building science has been co-ordinated by the CIB and its Working Commission on Rain Penetration. This Commission commenced its work in 1953 and united building research institutes throughout the world: (in alphabetical order) Belgium, Canada, Denmark, France, German Federal Republic, Hungary, India, the Netherlands, Norway, Rumania, South Africa, Spain, Sweden, the United Kingdom and the former USSR [133, 134]. At symposia and meetings, the importance of free WDR measurements to be conducted at free weather stations was stressed (since WDR is not routinely measured at weather stations as opposed to horizontal rainfall). The Commission recommended the use of the 4-way WDR gauge constructed by Holmgren. Other improved free WDR gauges were conceived and tested by the Commission members, and several gauge intercomparisons were made (by Lacy in 1958 and 1964 [135-137] and by Korsgaard and Madsen in 1962 and 1964 [126-129]). The observed differences between gauge readings were attributed to differences between the exposure of the gauges [136, 137]. Lacy [138] stated that

> *"Although it is probably preferable to standardize the type of gauge used, the comparisons which have been made suggest that the results obtained will not be much affected by the choice of gauge."*

And in a general report for the Commission in 1965, Birkeland [93] concluded that all gauges catch about the same amount of WDR. These findings, together with the fact that WDR gauges were not industrially manufactured and WDR was not systematically measured by meteorological instances, were probably the cause that no definite standard for the design and use of WDR gauges was set. As a result, the CIB recommendations were soon abandoned. Research institutes and universities designed, manufactured and used their own WDR gauges - even today this is still the case. Table 1 summarizes all countries - of which the authors are aware - where WDR measurements with free-standing gauges have been performed for use in building science. These measurements have led to the joint conclusion that the intensity of free WDR increases approximately proportionally with wind speed and horizontal rainfall intensity. This in turn has led to the development of semi-empirical formulae as will be discussed in section 4 of this paper.

3.1.2. Wall-mounted wind-driven rain gauges

The first WDR gauge for measurements on buildings was probably that employed by Holmgren in 1937 in Trondheim, Norway. Later, in 1943, Nell positioned two WDR gauges at the facade of his house in Voorschoten, the Netherlands [166]. Their example was followed by many researchers in other countries. The gauges used were all of a similar basic design (Fig. 6). It were plate-type gauges consisting of a collection area and a reservoir. The collection area is made up of a shallow tray (collection plate or catch area) of some material, shape and size and is fixed at the building surface. It has a raised rim around the perimeter to prevent the collection of water from outside the plate. The lowest point of the tray is drilled and tapped to accept a tube leading to the reservoir. The volume or weight of the collected rainwater in the reservoir is manually or automatically registered at regular intervals.

As in free WDR research, a large part of the research concerning wall-mounted gauges was carried out by members of the CIB. For wall-mounted measurements, the CIB Working Commission on Rain Penetration recommended the use of the WDR gauge designed by Croiset in 1957 at the CSTB, France [133, 134]. This gauge is illustrated in Fig. 7. It is a “recessed” plate-type gauge, meaning that the collection area is to be built into the wall. The advantage of this type of gauge is that the disturbance of the wind field around the gauge is limited. The recession however is responsible for some inconvenience, as it imposes restrictions on the locations where it can be installed. As stated by Hendry [167] and Lacy [138], it can be used when there are windows in suitable parts of the buildings or if holes can easily be cut. When this is impossible, gauges must be mounted on the surface of the building. Intercomparisons between plate-type gauges were reported by Hendry [167] and by Lacy [138]. Although some occasional discrepancies were observed, no further attention was given to these, as readings appeared similar on the whole. As a result, most researchers abandoned the concept of recessed gauges and designed their own gauges, giving rise to a broad spectrum of existing gauges of different materials, shapes and sizes. To the knowledge of the current authors, WDR measurements on building facades have been and/or are being conducted in the countries and have been reported by the researchers listed in Table 2. Photographs of recessed and non-recessed WDR gauges are given in Fig. 8. Measurements by wall-mounted gauges have revealed several features of what is nowadays called the “classic” wetting pattern of building facades: (1) The

windward facade is wetted whereas the other facades remain relatively dry. (2) At the windward facade, the wetting increases from bottom to top and from the middle to the sides. Typically, the top corners are most wetted, followed by the top and side edges. (3) For high and wide buildings, most of the windward facade only receives little WDR, except for the corner and the top and side edges. (4) The WDR intensity at a given position increases approximately proportionally with wind speed and horizontal rainfall intensity. In conclusion of this section, it is noted that the gauges that were originally designed to be wall-mounted, were soon also used for free WDR measurements (thus only yielding information for one selected wind direction, unlike the original 4-way, 8-way, circular or tube-shaped free-standing WDR gauges).

3.2. Accuracy of wind-driven rain measurements

WDR gauges are not industrially manufactured and there exists no standard on their design. As a result, there are almost as many types of WDR gauges as there are researchers using them. The present discussion is focused on the plate-type WDR gauges that are used for measurements on buildings. The reasons are: (1) the fact that most gauges used are plate-type gauges, whether they are wall-mounted or free-standing, and (2) the fact that the discussion of these gauges will for a large part be extendable to the traditional 4-way, 8-way and - to a lesser extent - circular and tube-shaped WDR gauges. The individual plate-type gauges differ by material, shape and size of the collection plate. In the past, little attention has been given to the influence of these differences on gauge accuracy and performance. Comparative studies were undertaken by Hendry in 1964 [167] and by Lacy [138] in 1965. They found some occasional discrepancies but no large differences on the whole. In 1977, a comparative study by Meert and Van Ackere [168] at the Belgian Building Research Institute (BBRI) indicated the form of the gauge to have some influence. Recent comparative studies were conducted in 1998 and 1999 by Kragh [176], Högberg [205, 206] and Högberg et al. [193] in a joint research project of the Building Physics groups of the TUD, Chalmers University of Technology (CTH) and the Technical University of Eindhoven (TUE). These tests included, for the first time, gauges that were specially designed to measure adhesion water. During and after a WDR spell, there is always an amount of water (individual drops or water film) adhered to the collection area. This amount is not collected in the reservoir and hence not measured. After and to a lesser extent also during the spell, this *adhesion water* evaporates. Kragh [176] at the TUD developed a WDR gauge that deviated from traditional gauges in that it is suspended from a load cell, allowing both the collected amount of WDR in the reservoir and the amount of drops adhered to the gauge surface to be registered (Fig. 9). Van Mook [192] at the TUE designed a WDR gauge that is equipped with an automated wiper to collect the adhesion water from the collection area (Fig. 10). The comparative studies by these authors indicated that these gauges could collect up to twice the amount of WDR that was measured by their ordinary counterparts [193], on short (hourly) as well as on long (monthly) time bases. Based on this observation, Kragh [176] and Högberg et al. [193] identified adhesion water evaporation as the major error source. It should be mentioned that these large errors were found for traditional gauges with hydrophobic PTFE surface finish. Traditional PMMA gauges performed better, indicating the presence of lesser adhesion water at this surface.

Recently, a model was developed by the current authors to estimate the adhesion-water-evaporation error in WDR measurements [175]. The model simulates the behavior of drops impinging on gauge collection areas including adhesion, coagulation and run-off. Fig. 11 presents simulation results for one of the traditional (i.e. without load cell suspension or automated wiper) gauge types that were designed at the Laboratory of Building Physics, Katholieke Universiteit Leuven (KUL). The gauge will be referred to as KUL. It has a 0.3x0.3 m² rectangular collection area made of PVC. The figure illustrates the distribution of the amount of applied WDR between the collection area (adhesion water) and the reservoir for different applied WDR amounts. The dotted line in Fig. 11 is the sum of collected and adhesion water. It indicates the amount of WDR that would be caught by an ideal gauge. The amount of water caught by traditional gauges however is less (dashed line). The solid line "adhered water" is a measure for the possible adhesion-water-evaporation error at different total impinged WDR amounts, assuming no evaporation during the spell and total adhesion water evaporation after the spell. The model was verified by comparison with laboratory experiments. Although model and experiments do not quite agree between 0.08 mm and 0.18 mm, the main observation is the existence of two situations: (1) for WDR amounts smaller than about 0.08 mm, the measurement error is 100% (all impinged water is adhered to the surface); (2) above this threshold, the absolute measurement error can be considered constant (here: about 0.08 mm and hence the relative measurement error decreases as the collected amount of WDR during the spell increases). For other gauge types (i.e. other material, shape and size of the collection area) similar qualitative but different quantitative results will be obtained. Further studies for e.g. PTFE gauges are currently in progress, indicating that using hydrophobic surface finish increases the measurement errors, rather the contrary of what has been assumed in the past. Similar remarks have been made by Högberg et al. [193] and Högberg [109].

Other error sources are considered to be of lesser importance [175, 185, 193] but cannot be excluded. They comprise (1) evaporative losses from the reservoirs, (2) splashing of raindrops from the collection area, (3) condensation on the collection area and (4) wind errors, meaning smaller catches due to the disturbance of

the wind flow by the gauge body. Evaporation from the reservoirs can be measured and is small during rain (high relative humidity). It can be retarded by regularly adding a few drops of light oil in the reservoirs [217]. Splashing refers to the collision of a water drop on a solid surface. This phenomenon is extremely complex and many factors are involved. Most of this research has been conducted in other research domains and has been concerned with the impact of vertically falling drops on horizontal or inclined surfaces. Research of splashing on vertical surfaces has to our knowledge only been performed by Couper in 1974 [140] and by Högberg between 1998 and 2002 [109, 204-206]. Högberg at CTH developed a WDR gauge with a deeply recessed collection area composed of tilted surfaces to avoid splashing losses (Fig. 12). It was found that the performance of this gauge was better than that of non recessed gauges for high wind speed and heavy rainfall intensities (large raindrops), whereas the large collection area increased the evaporative losses that dominated performance for light to moderate rainfall intensities. Condensation errors are expected to be small for all gauge types. The typical condensation with nocturnal infrared loss on a vertical surface on a clear night is of the order of a few tenths of a millimeter [218]. If significant, it can easily be eliminated if measurements are taken with a sufficiently high temporal resolution by comparing the WDR measurements with measurements of horizontal rainfall. Wind errors are expected to be less important for wind directions that are approximately perpendicular to the collection area, given the small wind speed that exists near the surface. For sharp wind angles, higher wind speed values exist near the surface and the influence of the rim of the gauge will become more important. It causes a deformation of the wind flow and the raindrop trajectories. A solution that has been suggested is the use of recessed gauges. But, even then, local changes in the wind flow pattern occur near and inside the gauge. Further research is needed to identify this type of error. Finally, it is noted that already in the design of the free-standing 4-way and 8-way WDR gauges, splashing was minimized by the use of deep collection area surfaces. These gauges however cause an important distortion of the free wind flow field. The circular and tube-shaped gauges by Korsgaard and Madsen were designed for lesser wind distortion, and their superior performance has been confirmed by comparative measurements [128]. Choi designed a WDR tower similar to the free-standing 4-way WDR gauge, but with an additional feature to reduce the flow field distortion by the tower. Flow paths inter-connecting the 4 vertical openings were provided so that the wind can blow through the tower [130-132].

3.3. Application

WDR measurements are presented that have been conducted on the south-west facade of the low-rise VLIET test building in Heverlee, Leuven (KUL) by Blocken and Carmeliet [174]. The building consists of two main modules, the flat roof module and the sloped roof module. In between the main modules, there is a small terrace module (Fig. 13a). Building dimensions including roof overhang length are illustrated. Roof overhang varies along the length axis of the building as indicated. The direction of the prevailing winds at the test site is south-west. For the purpose of WDR studies, one of the longitudinal facades of the building was constructed facing this direction. The building is situated in a suburban area. For the south-west facade, the only elements providing some shielding from wind and rain are a row of poplars at the north-west side and some low agricultural constructions that are situated about 80 m in front of the south-west facade. Meteorological data (wind speed U_{10}, wind direction φ_{10}, horizontal rainfall amount S_h) are gathered on site and upstream of the south-west facade by an automatic weather station measuring on a 10-minute basis. In addition, 9 WDR gauges type KUL (0.3x0.3 m² catch area) are positioned on the facade. Fig. 14a displays the meteorological data record for the period 1-5 January 1998. The wind direction during the rain event is approximately perpendicular to the south-west building facade (225° from north). The quantity of WDR collected by the gauges at the end of the rain event is given in Fig. 13b (catch ratio values). Multiplying the catch ratio with the horizontal rainfall amount for the rain event (S_h = 24.8 mm) yields the WDR amount. The 9 measurement values reveal part of the spatial distribution of WDR across the facade. The highest amount occurs near the flat roof module edge. The smallest WDR amount on the south-west facade is collected by gauge 1, due to shelter by roof overhang. Focusing on gauge 7, Fig. 14b yields the temporal distribution of cumulative 10-minute collected WDR amounts during the rain event. Comparing with Fig. 14a, it is obvious that the highest WDR amounts occur during the co-occurrence of higher wind speed and peak rainfall intensities. Assuming a worst case scenario, meaning complete adhesion water evaporation after each separate spell in the rain event and employing the information from Fig. 11, an estimate for the adhesion-water-evaporation error is 13x0.08 mm = 1.04 mm. For the catch ratio at the end of the rain event: estimate of absolute error e = 1.0 mm/24.8 mm = 0.04. The (worst case estimates of the) relative errors for this rain event are rather small due to the choice of rain event (large amount of WDR) and the type of WDR gauge (PVC surface finish performing better than PTFE). These error estimates would even be smaller if the rain event was not composed of so many individual rain spells that are separated by dry periods. The wind direction is approximately perpendicular to the south-west facade and the gauge rim is only 0.01 m, hence wind errors are expected to be small. Evaporation losses from the (outside) reservoirs (long rainy period) and splashing losses (small rainfall intensities and low wind speed) are considered negligible.

3.4. Physical simulation of wind-driven rain in wind tunnels

The possibility of wind tunnel modeling of WDR on buildings has been considered by Flower and Lawson in 1972 [219] and by Rayment and Hilton in 1977 [220]. They mentioned the difficulties involved. Flower and Lawson concluded that it should be possible to predict impingement rates on buildings by suitable laboratory tests. Rayment and Hilton visualized the movement of raindrop trajectories around a building model using bubbles. Only two actual attempts of WDR quantification tests are known to the authors. An elaborate scaled wind tunnel simulation has been performed at the Boundary Layer Wind Tunnel Laboratory by Inculet and Surry [221-223]. Modeling of WDR on a full-size building has been attempted in the large Jules Verne wind tunnel at the CSTB-Nantes [224-225]. The wind tunnel simulation by Inculet and Surry will be briefly discussed here. Nozzle arrays were installed in a boundary layer wind tunnel. Building models at a scale of 1:64 were constructed and placed in the wind tunnel. The wind speed and the raindrop sizes were scaled and WDR on the buildings was physically simulated. An important problem was determining the amount of WDR falling onto different positions on the models. Measuring WDR on small models requires the use of special techniques such as the electrostatic-sensor technique or the water-sensitive paper method (Inculet and Surry 1994). In these experiments, the water-sensitive paper method was used. This method consists of positioning pieces of water-sensitive paper on the building model. Each drop that falls on the paper leaves a stain. This way, a visual picture of the wetting pattern is obtained. These tests clearly reproduced the "classical" wetting pattern of building facades. Based on these wetting patterns, by counting and sizing each individual stain, an estimate of the amount of WDR falling onto different parts of the model was determined (Inculet and Surry 1994). However, a number of difficulties were associated with the experiments. These were accurately described by Inculet and Surry (1994). They reported that the major drawbacks are the very limited time of the rain shower (individual drops must remain distinguishable on the paper) and the fact that the quantitative analysis (counting and sizing of individual stains) is very labor-intensive and therefore not possible for all locations and for a large number of tests. It was also mentioned that the short duration of the tests (5 to 10 seconds) might result in a considerable variability from test to test. Another difficulty was providing a spatially uniform distribution of rain from the nozzles (meaning that in an empty wind tunnel, the nozzle arrays should provide a uniform horizontal rainfall intensity and a uniform raindrop size distribution pattern on the wind tunnel floor). While field work has its own specific requirements, wind tunnel work appears to be no less demanding: it is labor intensive, expensive and suffers from a number of important problems and restrictions (Surry et al. [221], Inculet and Surry [222] and Gandemer [225]). Whereas it was hoped that the accuracy of wind tunnel data would be higher than field data, the two wind tunnel experiments mentioned above indicated that this is not necessarily true. Problems that will require specific attention in future wind tunnel modeling are the simulation of a spatially uniform drop size distribution and the development of techniques for determining the impinging quantity of WDR on small-scale building models.

3.5. Discussion

- The methods for field measurements of WDR in building science have practically remained unchanged since the first measurements were made in the 1930s. In contrast to the very simple measurement principle, determining the error of the measurements appears to be complicated. Evaporative loss of adhesion water from the collection area is considered to be the most important error source. This error can be very large. The relative adhesion-water-evaporation error of WDR measurements decreases as the collected amount of WDR increases.
- Measurements of both free WDR and WDR on buildings have indicated that the intensity of WDR increases approximately proportionally with wind speed and horizontal rainfall intensity. Measurements of WDR on buildings have revealed part of the complex wetting pattern of a facade: top corners, top and side edges are most exposed to WDR.
- A systematic experimental approach in WDR assessment is not feasible. WDR is usually not measured at meteorological stations and databases of WDR field measurements are not commonly available. Furthermore, WDR measurements usually only provide limited spatial and temporal information and measurements at a particular station have very limited application to other sites. Wind tunnel measurements are very demanding. They are labor intensive, expensive and difficult and the latter factor negatively influences their accuracy. Note that this is the present status of wind tunnel modeling reported in literature and that future research efforts might lead to new techniques yielding improved simulations with a higher accuracy.
- Despite all drawbacks mentioned, the experimental method has proven vital in gaining knowledge on the interaction between WDR and buildings. Field measurements serve as a basis for the development and validation of semi-empirical methods and for the validation of numerical methods. The restriction, which

has to be kept in mind when using and interpreting such measurement results is that – depending on gauge type and duration, intensity and type of the rain event - errors can be very large (any value up to 100%).

4. Semi-empirical methods

Standard meteorological data measured at weather stations are wind speed, wind direction and horizontal rainfall. WDR is usually not measured. It would therefore be interesting if the WDR exposure of building facades could be obtained from standard weather data. This drove researchers to establish semi-empirical relationships between the quantity of WDR and the influencing climatic parameters wind speed, wind direction and horizontal rainfall. The development of the relationships was guided by the experimental observations that both the free WDR and the WDR on buildings increase approximately proportionally with wind speed and horizontal rainfall. The formulae are semi-empirical in that their forms have theoretical bases but free parameters have been chosen to fit experimental data. Practically all existing semi-empirical methods are based on one of two approaches, both of which were initiated by Hoppestad in 1955 [124]: the WDR index and the WDR relationship.

4.1. The wind-driven rain index and wind-driven rain maps

The concept of the WDR index originated from the observation that the product of wind speed and horizontal rainfall amount appeared proportional to the amount of WDR. Calculating this product (the WDR index) for a variety of places throughout a country, WDR maps were constructed. The first WDR map was made by Hoppestad in 1955 [124] for Norway based on WDR measurements by the 4-way free WDR gauge (Fig. 4b) and on standard meteorological data. This map provides direct estimates of the amount of free WDR. Other maps were constructed on the basis of the WDR index. In 1962, Lacy and Shellard [226] published WDR maps for the British Isles based on an annual WDR index (product of annual values of wind speed and horizontal rainfall amount). Lacy [138] recognized the limitations of the WDR index:

> *"No attempt was made to estimate the actual amount of WDR. This amount would depend very much on the disturbance to air flow caused by whatever was receiving the rain."*

but he stressed the qualitative importance of this measure [66]:

> *"The annual mean WDR index gives, it is believed, a reasonably precise method of comparing different sites with respect to total amounts of WDR on walls. It enables a designer to compare the exposure of a place with that at another with which he is already familiar."*

Omnidirectional and directional WDR maps of the UK that were published in 1971 are illustrated in Fig. 15 [227].

The WDR index approach was followed by a large number of researchers. New WDR maps for European countries were a main topic at the meeting of the CIB Working Commission for Rain Penetration in Madrid, 1966. Contributions from Denmark [228], Poland [229], Rumania [230], Spain [231] and West Germany [232] were received. Critically revising the WDR index approach in the same year, Künzel [233] concluded that, although valuable for the British Isles and Norway, the approach appeared insufficient for other European countries. In many cases the WDR index underestimated the actual WDR exposure. According to Caspar [232] this was caused by the fact that the WDR index was obtained using wind speed values that were averaged over periods with and without rain, instead of only averaging during rain. Frank (1973, [183]) attributed the differences due to this averaging deficiency to the different climatological and topographical circumstances in the other European countries. Other deficiencies of the WDR index approach were noted: (1) The use of long time averages (*annual* wind and rain data); (2) The fact that the WDR index is a long duration index. As it is based on averaged values, it is representative for long-term events such as moisture accumulation in porous materials but not for short-term events such as penetration through windows and curtain walls; (3) The WDR index relates to the free WDR and does not take into account local phenomena induced by the topography and the building itself. Improvements and further developments of the British WDR maps were made by Lacy in 1976 [234], by (Caton and) Prior in 1985 [235] and by Prior and Newman in 1988 [212], providing the basis for the BSI (British Standards Institution) Draft for Development 93 (BSI 1984, [236]). This draft was superseded in 1992 by BS 8104 "Code of practice for assessing exposure of walls to WDR" (BSI 1992, [237]). The improvements comprised: (1) The use of hourly wind and rain data in calculating the indices; (2) The introduction of a spell index alongside the average annual index to represent short duration WDR events; (3) The introduction of four empirical factors to take into account the effect of terrain roughness, local topography, obstructions and building geometry. This way, throughout the years, the WDR index method evolved from a

qualitative approach (comparing the WDR exposure from a particular location in respect to another) to a quantitative approach (actually determining free WDR amounts and WDR amounts on facades). It was recognized that using the four empirical factors constituted an important simplification of reality but that this was necessary to avoid complicating the standard too much [237]. To conclude the discussion of the WDR index, Table 3 presents an overview of countries for which WDR maps have been prepared. For completeness, it is noted that the British Standard BS 8104 was in 1997 converted into the European Standard Draft PrEN 13013-3 (CEN 1997, [238]), based on important work done by Sanders [239] in 1996. This Standard Draft is closely based on the BS 8104, but it combines the WDR index approach (explained in this section) and the WDR relationship (explained in the next section). Because of its importance, the European Standard Draft will be briefly explained in section 4.3.

4.2. The wind-driven rain relationship

The WDR relationship is based on a simple theoretical formula. If we assume that all raindrops are of the same size and that the wind flow is uniform, steady and horizontal, the intensity of WDR passing through an imaginary vertical surface can be expressed as [124, 127, 138]:

$$R_{wdr} = R_h \cdot \frac{U}{V_t} \tag{3}$$

where U is the wind speed (m/s) and V_t is the raindrop terminal velocity of fall (m/s). In Eq. (3), the wind direction is assumed to be perpendicular to the vertical surface at all times. It assumes no deflection of wind or raindrops by the vertical surface and hence is a measure for the free WDR. Hoppestad [124] proposed the following formula based on Eq. (3):

$$R_{wdr} = \kappa \cdot U \cdot R_h \tag{4}$$

He called Eq. (4) “the WDR relationship” and the factor κ “the WDR coefficient”. Average values for κ were obtained by measurements with the 4-way free WDR gauge at four different locations: Oslo ($\kappa = 0.130$), Bergen ($\kappa = 0.188$), Trondheim ($\kappa = 0.221$) and Tromsö ($\kappa = 0.148$), yielding an average value of 0.180. In search for a verification of his WDR index, Lacy [66,138] refined Eq. (4) by employing the empirical relationships that express the median raindrop size as a function of horizontal rainfall intensity [248] and the terminal velocity of fall of such raindrops [249]. This led to Eq. (5):

$$R_{wdr} = 0.222 \cdot U \cdot R_h^{0.88} \approx 0.222 \cdot U \cdot R_h \tag{5}$$

where 0.222 (s/m) is the WDR coefficient (average value) that results from the adopted empirical relationships. The exponent 0.88 can in good approximation be omitted. Several researchers measured free WDR amounts, finding a good agreement with results calculated with Eq. (5) [127, 128, 138, 152, 154]. Comparing Eq. (3) with Eq. (4) and Eq. (5), we note that the WDR coefficient is the inverse of the raindrop terminal velocity of fall. Eq. (5) therefore implies that an average spell can be considered as composed of all similar sized drops with V_t = (1/0.222) m/s = 4.5 m/s, corresponding to a raindrop diameter of 1.2 mm. This is a realistic value for spells of light to moderate intensity [250]. From measurements and a literature review, Straube and Burnett [112] have found the WDR coefficient to range between 0.20 and 0.25 s/m for average conditions, but considerable variations to occur for different horizontal rainfall intensities and rain storm types: from more than 0.5 s/m for drizzle to 0.1 s/m for intense cloudbursts. Relating the WDR coefficient to the raindrop terminal velocity of fall, WDR coefficients of 0.5 s/m and 0.1 s/m refer to 0.5 mm and 5 mm diameter drops respectively.

Eq. (5) yields the amount of WDR passing through a vertical surface in an undisturbed air stream. It does not take into account local phenomena induced by the topography and by the building itself. The particular wind flow pattern around a building causes deflection of the wind and of the raindrop trajectories. As a result, the amount of WDR on buildings can widely differ from the free WDR. Accounting for local effects was attempted by a relationship similar to Eq. (5), using an adapted WDR coefficient α (Eq. (6)):

$$R_{wdr} = \alpha \cdot U \cdot R_h \cdot \cos\theta \tag{6}$$

where θ is the angle between the wind direction and the line normal to the wall. This equation is the WDR relationship for WDR on buildings. The weakness of this method is the determination of the adapted WDR coefficient, as the entire complexity of the interaction between WDR and the building is to be integrated in this

single value. Künzel [251] correctly stated that WDR coefficients for positions on a building must either be determined by short-term measurements or estimated from experience (in turn based on measurements), as long-term measurements would take too much time. In spite of this, the factor should reflect an average value, i.e. averaged over several rain events. Measurements by Lacy [138], Ishizaki et al. [187], Schwarz [182], Sandin [200], Henriques [159], Flori [151], Künzel [153], Hens and Ali Mohamed [171], Straube and Burnett [112] and others indicate that WDR coefficients vary considerably with the size of the building and show a large variation across the building facade: values from 0.02 s/m (9% of 0.222) to 0.26 s/m (120% of 0.222) have been found. It must be emphasized that the value $\kappa = 0.222$ s/m is a theoretical value valid for free field conditions only (no building present). For assessing the amount of WDR on buildings, Eq. (6) with the appropriate value for α should be used. There is some confusion about this in the literature. Often Eq. (5) is used to predict the WDR amount on building facades.

4.3. The European Standard Draft PrEN 13013-3

In this section, the European Standard Draft (CEN 1997, [238]) is briefly explained to illustrate its capabilities and its deficiencies. The European Standard Draft is for a large part similar to the British Standard BS 8104 (1992), which was based on a long series of WDR measurements on buildings at a large number of locations within the UK. The Standard Draft provides a procedure to analyze hourly weather data (wind speed, wind direction, horizontal rainfall amount) in order to obtain an estimate of the quantity of WDR that impacts on a building wall of any given orientation. Following this procedure, two quantities are computed: (1) The annual average index (as a measure for the moisture content of masonry) and (2) the spell index (as a measure for the likelihood of rain penetration through masonry). The Standard Draft comprises two steps: (1) The calculation of airfield indices; (2) The calculation of wall indices.

4.3.1. Calculation of airfield indices

The airfield index is defined as the quantity of WDR that would occur during one hour at a height at 10 m above ground level in the middle of an airfield, at the geographical location of the wall. (Note that this is the "free" WDR that was mentioned earlier, as it would be collected by a free-standing WDR gauge when there are no obstructions for the wind flow). A distinction is made between the airfield annual index (I_A) and the airfield spell index (I_S). Both indices are calculated based on Eq. (5) multiplied with the factor "cosθ". The airfield annual index is the airfield index for a given direction totaled over one year. The airfield spell index is the airfield index for a given direction totaled over the worst spell likely to occur in any 3-year period. The calculation is performed with at least 10 (and preferably 20 or 30) years of hourly values of wind speed, wind direction and horizontal rainfall from the nearest meteorological station.

4.3.2. Calculation of wall indices

To take into account the difference in exposure between the "airfield situation" and the "building situation", correction factors are introduced to convert the airfield indices to wall indices (i.e. the quantity of WDR that would fall onto a real building wall). The correction factors are (1) the terrain roughness factor R, (2) the topography factor T, (3) the obstruction factor O and (4) the wall factor W. Multiplying the airfield annual index and the airfield spell index with these correction factors respectively yields the wall annual index (I_{WA}) and the wall spell index (I_{WS}) (Eqs. (7) and (8)).

$$I_{WA} = I_A \cdot R \cdot T \cdot O \cdot W \tag{7}$$

$$I_{WS} = I_S \cdot R \cdot T \cdot O \cdot W \tag{8}$$

The terrain roughness factor takes into account the variability of the mean wind speed at the site due to the height above the ground and the upstream roughness of the terrain. The topography factor takes into account the increase of the mean wind speed over isolated hills and escarpments. The obstruction factor takes into account the shelter of the wall by the nearest obstacle of similar dimensions to the wall that is situated in front of the wall (e.g. another building, trees). Finally, the wall factor tries to take into account the type of the wall (height, roof overhang) and the variation of the WDR over the surface of the wall. The roughness factor and the topography factor are determined from formulae with appropriate parameters. The former is dependent on the height above ground. At e.g. 2 m above ground, it ranges from 0.76 for urban areas to 0.90 for smooth, flat terrain without obstacles. The topography factor ranges between 1.00 for upstream slopes with less than 5% inclination to a peak value of 1.36 for buildings situated at the crest of steep cliffs or escarpments. The obstruction factor is determined from Table 4, where the distance of the obstruction from the wall refers to the horizontal distance of

the wall to the nearest obstacle of similar dimensions to the wall along the line of sight from the wall. It is noted that the obstruction factor may vary significantly at different points along a long wall. To determine the wall factor, the Standard Draft provides a table with figures. This information is reproduced here as Fig. 16. It is noted that mainly information for low-rise buildings is provided. This is most likely due to the fact that the Standard Draft was written with masonry walls in mind. It is important to note that, in the procedure of the Standard Draft, the product of the free WDR coefficient (0.222 s/m, which is used in the calculation of the airfield index) with the correction factors R, T, O and W is made (which is additionally multiplied with wind speed and horizontal rainfall data). This product is in fact the "adapted WDR coefficient α", which has been mentioned in section 4.2. (Eq. 6).

4.4. Other developments

Many researchers have built further on the WDR index and the WDR relationship. Some of the developments are briefly referenced here. For further information, the reader is referred to the original research publications. It is noted that both approaches are closely related (in fact, the product $U.R_h$ in the WDR relationship is the WDR index) and that some developments are built on their combination. WDR indices have been calculated by, among others, Morris [252] and Sneyers et al. [253]. Efforts to correlate the qualitative WDR index (as originally defined by Lacy: product of annual rainfall and annual mean wind speed) and the amount of free WDR were undertaken by Henriques [159] and in more detail by Choi [254]. Choi [99, 132] also performed studies to correlate the WDR index and the WDR amount and intensity on buildings. Further WDR index developments are attributed to Fazio et al. [255] and Zhu et al. [256, 257]. They computed WDR impact frequency and impact duration in addition to WDR intensity for a large number of Canadian cities. Improvements to the quantitative WDR index approach (British Standard 8104) were suggested by Hens and Ali Mohamed [171]. Sanders [239] developed a method closely related to the British Standard 8104 as the basis for the European Standard Draft. Kragh [176] and Högberg [109, 206] used Sanders' method to determine the WDR amount on buildings on short time bases. Underwood and Meentemeyer [245] constructed WDR maps for the United States that were no longer confined to WDR intensity but additionally provided information about WDR event duration, annual frequency, total receipt and direction.

A number of researchers have been studying the co-occurrence of wind and rain (without actually determining the WDR index or WDR amounts) to obtain a rough and qualitative idea of the WDR exposure of building facades. For completeness these studies are briefly mentioned here. In 1933, Thein [258] studied the co-occurrence of wind and rain as part of a research project concerning rain penetration of buildings in Hamburg, Germany. Other co-occurrence studies were conducted by Zobel [259], Linforth [260], Gordon [261], Robinson and Baker [79], Meert and Van Ackere [169], Sacré [262, 263], Sadagashvili and Kartvelishvili [264], Beguin [265], Murakami et al. [266], Choi [267], Tsimplis [268], Surry et al. [269], Flori [270] and Straube [147].

4.5. Accuracy

Semi-empirical methods can only be used to obtain rough estimates of the WDR exposure. Concerning the WDR index, BS 8104 (BSI 1992, [237]) itself states that it should be emphasized that neither index (annual average nor spell index) is precise enough to enable fine distinctions between degrees of exposure to be made and that the user should always take account of local knowledge and experience. Concerning the WDR relationship, the use of an accurate WDR coefficient α to determine the WDR exposure of building walls is essential. However, this coefficient depends on a large number of parameters: building geometry, environment topology, position on the facade, wind speed, wind direction, horizontal rainfall intensity, raindrop spectrum, type of WDR gauge used. An accurate WDR coefficient cannot be obtained from short-term measurements. Such values are only representative for the type of spell during the measurement. The measurements should comprise spells of different wind and rain characteristics to be representative. On the other hand, such long-term measurements will only yield estimates of average WDR exposure.

All semi-empirical methods are partly based on measurements that were conducted with traditional WDR gauges (i.e. no suspended or wiper-equipped gauges as discussed in section 3.2). Depending on the type of gauges and on the type of the rain spells, these measurements can exhibit significant errors (underestimations). Results from them should therefore be used with caution. It is possible that the present semi-empirical methods underestimate the WDR amount.

4.6. Discussion

- Standard meteorological data measured at weather stations are wind speed, wind direction and horizontal rainfall intensity. WDR is usually not measured. Therefore, it would be interesting if the WDR exposure of

building facades could be obtained from semi-empirical relationships between standard weather data and WDR exposure.

- The pioneering work of Hoppestad in Norway and Lacy in the United Kingdom has provided two semi-empirical methods: the WDR index and the WDR relationship.
- The WDR index is calculated as the product of wind speed and horizontal rainfall amount and is approximately proportional to the WDR amount. In its original form, it is a qualitative measure of the exposure of a location to the "free" WDR. Further developments and improvements in the past decades have transformed the index into a quantitative measure of the exposure of a building wall to WDR.
- The WDR relationship is a formula relating WDR intensity to the standard variables wind speed, wind direction and horizontal rainfall intensity by a WDR coefficient. The main problem when using this relationship is obtaining a reliable WDR coefficient, as it depends on a large number of parameters and is different for each situation and for each WDR spell. A WDR coefficient can be obtained by short-term measurements or by long-term measurements. The former will yield a WDR coefficient that is only representative for the WDR spell measured, the latter will yield a coefficient that is only representative for the average of the measured situations.
- The European Standard Draft provides a procedure that is based on both the WDR index and the WDR relationship. It inherently uses an adapted WDR coefficient α that is determined as the product of the free WDR coefficient (0.222 s/m) with four empirically determined correction factors, which can be selected by the user. The Standard Draft is the result of good research work over many years and it is based on a wide range of WDR measurements on different buildings and at various positions on these buildings. It is clearly superior to the traditional practice of using the WDR relationship with a single WDR coefficient that does not take into account the variation of WDR with the building geometry and with the position on the building facade. However, the Standard Draft also has a number of drawbacks: (1) It can only be applied for the building configurations shown in Fig. 16. (2) The wall factors in Fig. 16 only provide limited information about the spatial variation across the facade. (3) The WDR coefficient α is assumed to be constant for a fixed position on the building (i.e. constant in time). (4) It is assumed that the effect of varying wind direction can be taken into account by the factor $\cos\theta$ (cosine projection).
- The accuracy of semi-empirical methods has up to now not been investigated. It is not clear to what extent the underlying assumptions of the WDR relationship and the European Standard Draft (α constant in time, cosine projection) are justified.
- Semi-empirical methods can provide rough estimates of the WDR quantity to be expected on buildings. Such estimates may be sufficient in some cases, but they are insufficient when more detailed information is requested, e.g. the complete WDR distribution on buildings or the effect of building details such as roof overhang. In such cases, one has to resort to numerical methods.

5. Numerical methods

5.1. Numerical simulation of wind-driven rain

As research efforts employing experimental and semi-empirical methods continued to reveal the inherent complexity of the problem, researchers realized that further achievements were to be found through numerical analyses. Already in 1974, Sandberg [271] calculated the movements of raindrops around a building model based on a flow pattern obtained by wind tunnel modeling. Similar calculations were performed by Rodgers et al. in 1974 [272, 273], by Beijer in 1977 [163], by Rodgers in 1977 [274] and by Hilaire and Savina in 1988 [177]. Souster (1979, [275]) studied raindrop trajectories based on computed flow patterns around 2D buildings, introducing Computational Fluid Dynamics (CFD) in the area. CFD comprises the use of numerical techniques to obtain the wind flow pattern. The bulk of numerical WDR research was conducted in the past decade. The pioneering work of Choi, starting from 1991 [95-99, 276] has been the break-through for the use of numerical methods in WDR research. He developed a numerical method where the raindrop trajectories were calculated based on a steady-state 3D wind flow pattern [95, 96, 276]. In this method, the flow pattern is obtained by solving the 3D Reynolds Averaged Navier-Stokes equations, the continuity equation and the equations of the standard k-ε turbulence model. From the configuration of raindrop trajectories ending on the building facade and the raindrop size distribution, the specific catch ratio and the catch ratio (see Eq. (1)) can be calculated. This numerical simulation technique allows the determination of the spatial distribution of WDR on buildings under steady-state conditions of wind and rain, i.e. for a fixed, static value of wind speed, wind direction and horizontal rainfall intensity (Choi [95, 96, 276]). These publications and following contributions considerably extended the existing knowledge [87, 100-106, 111, 277-283, 284]. In 2000, Blocken and Carmeliet [172-173] extended Choi's simulation technique by adding the temporal component and by developing a new weighted data averaging technique, allowing the determination of both the spatial and temporal distribution of WDR. Few attempts have been made for experimental validation of the numerical simulation technique. Lakehal et al.

(1995, [283]) compared numerical simulations for a street-canyon with experimental data for buildings of similar geometry. Van Mook (1999, [104, 105]) was the first to compare numerical simulations on a building with the corresponding full-scale measurements for selected 10-minute intervals. Hangan (1999, [282]) compared numerical simulations with the wind tunnel experiments that were carried out by Inculet and Surry [222, 223]. These research efforts focused on single stationary rain events, i.e. single intervals with a fixed, static value of wind speed, wind direction and horizontal rainfall intensity. Blocken and Carmeliet (2002, [174]) performed a validation study for WDR simulations on a low-rise test building in both space and time for a number of transient rain events, finding a good agreement between the numerical results and the corresponding WDR measurements. Instead of solving the complex 3D Reynolds Averaged Navier-Stokes equations, some researchers have employed the assumption of irrotational (i.e. potential) flow in their simulations [107, 108, 109, 285].

It was already mentioned in this paper that WDR research is of importance in many research areas but that so far, no exchanges could yet be noted. However, one exception that must be mentioned here is the recent numerical research work of Choi [286]. This author investigated the effect of WDR on the soil detachment on hill slopes, hereby applying the numerical techniques that he introduced earlier in building science to an important research subject in the earth sciences.

5.2. Accuracy

Several aspects are of importance in obtaining accurate CFD simulation results of WDR: the choice of the turbulence model, the resolution of the computational grid, the raindrop size distribution, the drag coefficient formulae, whether or not to include turbulent dispersion of raindrops and the time resolution of the input meteorological data.

The reliability of CFD calculations largely depends on the choice of the turbulence model. As mentioned by Versteeg and Malalasekera [287]:

"The results generated by a CFD code are at best as good as the physics embedded in it…"

Most CFD simulations of WDR have employed the standard k-ε turbulence model. In a recent publication addressing recommendations on the use of CFD in wind engineering [288], the use of more advanced models like the RNG model and the realizable k-ε model is recommended. The latter model is the one that has been used for the simulations in the WDR validation study [174], part of which will be presented in the next section. The realizable k-ε model is a modified version of the standard k-ε model. The term “realizable” refers to mathematical constraints on the normal stresses that are satisfied by the model: positivity of normal stresses and Schwarz inequality for shear stresses. The realizable k-ε model has been validated for a wide range of flows including separated flows and has been found to perform substantially better than its standard counterpart [289, 290].

Apart from the choice of turbulence model, numerical results are highly dependent on the computational grid that is constructed by the user of the CFD code [291-293]. The grid resolution should be high enough in order to capture the specific flow phenomena that occur around the building. However, grids should not contain too many nodes as this will require large computational resources and long calculation times. Grid sensitivity analysis should be performed in order to obtain a suitable grid that is a compromise of these two requirements. It comprises calculations with a number of different grids that are gradually refined (i.e. the number of nodes is increased) until a grid is found that yields results (in the region of interest) that no longer show a large dependence on the resolution of the grid.

Raindrop size distributions are usually not measured at weather stations. These measurements are complex [294-296] and such data is not generally available. Therefore, information on raindrop size spectra for the purpose of WDR simulations is usually obtained from empirical formulae [250, 297, 298]. In most cases, the formula of Best [250] has been adopted. This choice is based on the extent of the study carried out by Best. The study was supported by a wide bibliographical survey and measurements for a large number of rain events. The raindrop size distribution of Best exhibits a one-to-one relationship with horizontal rainfall intensity, which allows it to be unambiguously defined by the measured horizontal rainfall intensity values. A systematic investigation of the influence of different raindrop size distributions on the simulation results has not yet been performed. According to a number of studies by Choi [95-97] and by Blocken and Carmeliet [174], the sensitivity of the results to the raindrop spectrum appears to be rather small.

Drag coefficient formulae for spherical particles [299] are often used in raindrop trajectory calculations. However, as falling raindrops deviate from the spherical shape [300] these drag coefficients are an underestimation of the real ones, especially at high relative Reynolds numbers. High relative Reynolds numbers (referring to the airflow around an individual raindrop) are found in the case of large raindrops and/or a large difference between wind and raindrop velocity. Appropriate drag coefficients for falling raindrops were

measured by Gunn and Kinzer [301]. These are generally not included in commercial CFD packages. The deficiencies involved have been studied by van Mook [106].

The need for modeling turbulent dispersion of raindrops in WDR simulations remains an issue of disagreement amongst researchers. Lakehal et al. [283] evaluated three turbulent dispersion models to determine the WDR distribution in a street-canyon. Although the turbulent dispersion effect appeared weak for all but the smallest raindrops, it was demonstrated that it can be important in some special cases (e.g., buildings completely shadowed by others giving rise to very weak upstream wind flow patterns). Sankaran and Paterson [280, 281] conducted simulations on a single high-rise building. They found a very large influence of turbulent dispersion when looking at the WDR amounts on large areas at the windward facade. With a similar building configuration and also considering large areas at the windward facade, Etyemezian et al. [87] found the effect of turbulent dispersion to be small. Choi [98] performed simulations for a 40x40x40 m³ building studying the effect of small uncorrelated gusts (0.1 s gust period) and large correlated gusts (3 s gust period). For both gust types a small influence on the mean (i.e., time averaged) WDR amounts on the windward facade of the building was found. For large correlated gusts however a significant effect on the standard deviation of the time fluctuation of the WDR amount was observed. On the other hand, the calculations by van Mook [106] on a high-rise building indicate a considerable influence of turbulent dispersion on the mean WDR amount. Blocken and Carmeliet [174] demonstrated that an accurate determination of the WDR distribution on a low-rise building could be obtained without modeling turbulent dispersion. Comparing the results of the latter study with the results of Choi [98], it was thought that the use of 10-minute time steps by these authors represents a "mean" situation, as this frequency (1/600 Hz) is well below the bulk of gust frequencies in the micrometeorological peak of the wind speed power spectrum [302]. Turbulent dispersion has been neglected in the example numerical simulations in the following section.

Special attention is required for the climatic data used as input for the numerical method developed in Ref. [172]. It has been shown recently by the present authors that the use of hourly and daily values in WDR assessment can give rise to large errors, up to 80% [173]. Instead, short-term measurement data (e.g. 10-minutes or less) should be used. The use of hourly or daily data is only allowed when these data have been obtained by the conversion of high frequency data by a specific weighted averaging technique [173].

5.3. Application

5.3.1. Steady-state simulation technique [96]

The application of the steady-state numerical simulation technique developed by Choi is best illustrated by reproducing the results of a study published by this author in 1994 [96]. In a first step, the wind flow around a building 40 m high and 10 m wide by 10 m long was calculated with CFD. Closure was obtained by using the standard k-ε model. The wind speed inflow profile was a power law profile with an exponent 0.25 (suburban terrain). The inflow turbulence intensity was set at 10%. The wind flow pattern was calculated for reference wind speed values (at 250 m height) of 10, 20 and 30 m/s. The calculated flow pattern is illustrated in Fig. 17. The wind direction was perpendicular to the facade. Raindrop trajectories that were calculated based on the wind flow pattern are shown in Fig. 18 for the 10 m/s flow field and for two raindrop radii: very small (0.25 mm radius) and very large drops (5 mm radius). We briefly note here that the latter drop size is not realistic [300], but it serves the purpose of illustrating the influence of particle mass on the particle trajectories. Turbulent dispersion was not modeled. From these figures, it is clear that the trajectories of smaller raindrops are (1) more inclined and (2) more affected by the local flow pattern. Based on the configurations of the raindrop trajectories for each diameter in each wind flow pattern, the specific catch ratio was obtained (Eq. (1)). Given the specific catch ratio and using the raindrop size distribution of Best [250], values of the catch ratio (the ratio of WDR intensity to horizontal rainfall intensity) were obtained.

To study the WDR distribution across the building facade, it was divided into 12 large areas (3 vertical strips each one third of the building width and 4 horizontal rows each one quarter of the building height) (Fig. 19). The vertical side strips are named S (as both the building and the flow are symmetrical, the results of the two side strips are the same) and the center strip is named C. The horizontal rows are named 1 to 4 from bottom to top. The results as provided by Choi [96] are given in Table 5. The numerical results shown here are in general accordance with experimental observations reported earlier in this paper: the catch ratio increases with wind speed and a wetting pattern is found in which the top corners and the top and side edges are most exposed to WDR.

5.3.2. Spatial and temporal distribution of WDR and validation [174]

The extended numerical method developed by Blocken and Carmeliet is illustrated by employing it to determine the spatial and temporal distribution of WDR on the facade of the VLIET test building for the rain

event in Fig. 14a. The wind velocity field was obtained with the CFD package Fluent 5.4 [303]. The raindrop trajectories and the catch ratio results were calculated with author-written Fortran90 codes. The realizable k-ε model was used, calculations were performed on a computational grid with 906506 cells in a 200x90x40 m^3 computational domain, raindrop trajectories were calculated using the raindrop size distribution of Best [250] and the raindrop drag coefficients of Gunn and Kinzer [301]. Turbulent dispersion of the raindrops was not modeled. Short-term measurement data (10 minutes) was used as input. Further modeling and calculation details are found in [174]. The spatial distribution of the catch ratio at the end of the WDR event is given in Fig. 20. A distinct wetting pattern is found. Black areas indicate the facade positions that are sheltered by roof overhang. The highest catch ratio values are found near the vertical edges and near the unsheltered roof edge (terrace module). In addition to the contour lines, the calculated values at the positions of the WDR gauges are indicated. Most results agree fairly well with the corresponding measurement results given in Fig. 13b. However, the results at gauge positions 1 and 2 differ markedly. The catch ratio at these positions, especially at position 1, is most difficult to predict, because it is positioned on the transition region between sheltered and non sheltered area where a high wetting gradient is present (Fig. 20). In this region, a small shift in position yields a large shift in catch ratio value. The temporal distribution of WDR during the rain event is determined for gauge position 7 (Fig. 21). Although the calculations were performed with 10-minute values, for clarity, the results are only presented for hourly intervals. Measurements and calculations are in acceptable agreement, although an underestimation by the numerical method is to be noted. It is noted that the rain event was chosen for small measurement errors (high WDR amount) and was therefore suitable for model validation (absolute error on catch ratio values at the end of the rain event is 0.04: see section 3.3).

5.4. Discussion

- The complexity of the interaction between WDR and buildings has led to numerical modeling. The main part of numerical WDR research has been conducted in the past decade and has been made possible by the increasing computing performance.
- Numerical modeling has significantly increased the understanding of the interaction between wind, rain and buildings. The numerical method allows a detailed and high resolution quantification of WDR to be made, both spatially and temporally.
- Drawbacks of the numerical method are a very large amount of preparation work, the need for high computing performance (the more sophisticated calculations easily require up to 2 to 3 GByte RAM) and long calculation times.
- Accuracy requirements have been listed and must carefully be adhered to: the choice of the turbulence model, the spatial resolution of the computational grid, the raindrop size distribution, the drag coefficient formulae, whether or not to include turbulent dispersion of raindrops and the time resolution of the meteorological input data.
- The results of the few validation studies that have been performed are encouraging. Further validation studies for different building geometries and environment topologies are needed. Rain events for validation purposes must be carefully selected, in such a way that measurements errors are limited (e.g. high WDR amount, few evaporation periods, avoiding glancing wind angles, etc).

6. Conclusion

A comprehensive review of wind-driven rain research in building science has been presented. Experimental, semi-empirical and numerical methods for the quantification of WDR on buildings have been outlined. In conclusion:

- WDR measurements are rarely performed for other than research purposes. Being the primary tool in WDR assessment, they have provided the basis for semi-empirical methods and still serve as a basis for model development and model validation. It is important to realize that WDR measurements are not as easy as they might seem, as measurement errors can be large and depend on gauge type and rain event type.
- Semi-empirical methods offer a fast and easy approach to WDR quantification. They can only provide a rough estimate of the amount of WDR to be expected on building facades. While a semi-empirical assessment of WDR may be sufficient in some cases, it is of little interest when detailed information is requested.
- Numerical methods allow a detailed determination of the spatial and temporal WDR exposure at the expense of rather intensive preparation and calculation efforts. Numerical modeling is increasingly being used to study rain deposition patterns on buildings and to perform parametric analyses, exploring the effects of overall building geometry and geometric details on WDR loading [89, 90, 97, 106, 174, 282, 284].

It is the authors' opinion that the experimental method is not feasible for large-scale practical use in building design and hygrothermal analysis. Both the semi-empirical method and the numerical method have the potential of becoming a valuable tool in practical WDR assessment, provided that the drawbacks (for the semi-empirical method: not accurate enough; for the numerical method: too complex and labor intensive) are dealt with. In the near future one may expect a merging of the semi-empirical and the numerical approach into a joint quantification method. This might take the form of a "WDR exposure database" where adapted WDR coefficients for different buildings, environment topologies, positions on the building facade etc. are given that have been accurately calculated with a large number of numerical simulations. These coefficients can then be used in the easy-to-use WDR relationship to calculate the spatial and temporal distribution of WDR at the facade. The present authors are currently performing the establishment of such a database. Validating this new approach for practical use constitutes a challenge for the future.

Acknowledgements

Special thanks go to Michael A. Lacasse (National Research Council of Canada), Fabien van Mook (Eindhoven University of Technology, The Netherlands), Philippe Delpech (Centre Scientifique et Technique du Bâtiment – Nantes, France) and Alastair Stupart (Building Research Establishment - UK) for kindly completing our list of references with those manuscripts that were hard to come by. Appreciation is also expressed to Paul Peeters, KULeuven CBA Librarian, for the huge amount of work that he invested in collecting the major part of the manuscripts that are referenced in this paper. The graphical work in Fig. 4a, 8a and 15 is reproduced by permission of the BRE, Garston, Watford WD25 9XX, United Kingdom (copyright +44 (0)1923 664000). The graphical work in Fig. 17 and 18 is reprinted from Journal of Wind Engineering and Industrial Aerodynamics 51, E.C.C. Choi: "Determination of wind-driven rain intensity on building faces", pp. 55-69, ©2004, with permission from Elsevier. For the permission to reproduce photographs and drawings we thank the BRE, Elsevier, Vagn Korsgaard and Thomas Lund Madsen (Technical University of Denmark), Fabien van Mook, Anneli Högberg (Chalmers University of Technology) and Marcel Bottema (Rijkswaterstaat, The Netherlands). We thank the members of the International Micro Climate Group, in particular Fabien van Mook and Anneli Högberg, for valuable discussions and suggestions. We thank Hirozo Ishikawa (Tokai University, Japan), Mats Lyberg (Växjö University, Sweden), Carsten Rode and Britt Anderson (Technical University of Denmark) for their kind help in our search for literature. We are also indebted to all other researchers that provided us with their personal writings on the subject.

This research is funded by the Government of Flanders. As a Flemish government institution, IWT-Flanders (Institute for the Promotion of Innovation by Science and Technology in Flanders) supports and stimulates industrial research and technology transfer in the Flemish industry. Their contribution is gratefully acknowledged.

Appendix: List of symbols

Latin symbols

d	raindrop diameter
e	error in wind-driven rain measurement (catch ratio)
i, j	number of time step
I_A	airfield annual index
I_S	airfield spell index
I_{WA}	wall annual index
I_{WS}	wall spell index
O	obstruction factor
R	terrain roughness factor
R_{wdr}	wind-driven rain intensity
R_h	horizontal rainfall intensity (through a horizontal plane)
S_{wdr}	wind-driven rain amount
S_h	horizontal rainfall amount (through a horizontal plane)
t	time
T	topography factor
U, U_{10}	upstream horizontal wind velocity component at 10 m height
V_t	raindrop terminal velocity of fall
W	wall factor

Greek symbols

α	adapted wind-driven rain coefficient
Δt	time interval
η_d	specific catch ratio
η	catch ratio
θ	angle between wind direction and line normal to the wall
κ	(free) wind-driven rain coefficient
φ, φ_{10}	upstream wind direction at 10 m height

Abbreviations

BBRI	Belgian Building Research Institute (also WTCB in Dutch or CSTC in French)
BRE	Building Research Establishment (UK)
BRS	Building Research Station (UK), now BRE
BS	British Standard
BSI	British Standards Institution
CEN	European Normalization Committee
CFD	Computational Fluid Dynamics
CIB	International Council for Building Research, Studies and Documentation
CSTB	Center for Scientific and Technical Building studies (France)
CTH	Chalmers University of Technology (Sweden)
KUL	Katholieke Universiteit Leuven (Belgium)
LEF	local effect factor
LIF	local intensity factor
NBRI	Norwegian Building Research Institute
PMMA	polymethylmetacrylate
PTFE	polytetrafluorethene (Teflon)
PVC	polyvinylchloride
RAF	rain admittance factor
TNO	Netherlands Organization for Applied Scientific Research
TUD	Technical University of Denmark
TUE	Technical University of Eindhoven (The Netherlands)
VLIET	Flemish Impulse Programme for Energy Technology
WDR	wind-driven rain

References

[1] Hovind, E.L. 1965. Precipitation distribution around a windy mountain peak. J. Geophys. Res. 70 (14), 3271-3278

[2] Geiger, R. 1966. The climate near the ground. Harvard Univ. Press, 2nd printing of 1965 copyright edition, 611p.

[3] Sandsborg, J. 1970. The effect of wind on the precipitation distribution over a hillock. Nordic Hydrology 4, 235-244

[4] Sharon, D. 1970. Topography-conditioned variations in rainfall as related to the runoff contributing areas in a small watershed. Israel Journal of Earth-Sciences 19, 85-89

[5] Aldridge, R. 1975. The resultant direction and inclination of rainfall at Arahura Wairarapa, New Zealand. J. Hydrol. (New Zealand) 14, 55-63

[6] Poreh, M., Mechrez, E. 1984. The combined effect of wind and topography on rainfall distribution. J. Hydrol. 72 (1-2), 1-23

[7] Poesen, J. 1986. Field measurements of splash erosion to validate a splash transport model. Z. Geomorph. N.F., Suppl.-Bd. 58, 81-91

[8] Sharon, D., Morin, J., Moshe, Y. 1988. Micro-topographical variations of rainfall incident on ridges of a cultivated field. Trans. ASAE 31(6), (November-December 1988), 1715-1722

[9] Lentz, R.D., Dowdy, R.H., Rust, R.H. 1995. Measuring wind and low-relief topographic effects on rainfall distribution. Applied Engineering in Agriculture - ASAE. Vol. 11(2), 241-248

[10] Arazi, A., Sharon, D., Khain, A., Huss, A., Mahrer, Y. 1997. The windfield and rainfall distribution induced within a small valley: field observations and 2-D numerical modeling. Bound-Lay Meteorol. 83, 349-374

[11] Sharon, D., Arazi, A. 1997. The distribution of wind-driven rainfall in a small valley: an empirical basis for numerical model verification. J. Hydrol. 201, 21-48

[12] Bradley, S.G., Gray, W.R., Pigott, L.D., Seed, A.W., Stow, C.D., Austin, G.L. 1997. Rainfall redistribution over low hills due to flow perturbation. J. Hydrol. 202: (1-4) 33-47

[13] Reid, I. 1973. The influence of slope aspect on precipitation receipt. Weather 28, 490-494
[14] Hutchinson, P. 1970. A contribution to the problem of spacing raingages in rugged terrain. J. Hydrol., 12, 1-14
[15] Hayes, G.L. 1944. A method of measuring rainfall on windy slopes. Mon. Weather Rev. 72, 5, 111-114
[16] Pagliuca, S. 1934. The measurement of precipitation on a windy Mountain Summit. Trans. AGU 385-389
[17] Fourcade, H.G. 1942. Some notes on the effects of the incidence of rain on the distribution of rainfall over the surface of unlevel ground. Trans. Roy. Soc. South Africa 29(3), 235-254
[18] Hamilton, E.L. 1954. Rainfall sampling on rugged terrain. Tech. Bull. U.S. Dep. Agric., No. 1096, 41p.
[19] Sharon, D. 1980. The distribution of hydrologically effective rainfall incident on sloping ground. J. Hydrol. 46, 165-188
[20] De Lima, J.L.M.P. 1990. The effect of oblique rain on inclined surfaces: a nomograph for the rain-gauge correction factor. J. Hydrol. 115, 407-412
[21] Lacy, R.E. 1951a. Distribution of rainfall round a house. Meteorol. Mag. 80, 184-189
[22] Hayes, G.L., Kittredge, J. 1949. Comparative rain measurements and raingage performances on a steep slope adjacent to a pine stand. Trans. AGU 30(2), 295-301
[23] Heberden, W. 1769. On the different quantities of rain which appear to fall, at different heights, over the same spot of ground. Phil. Trans., 59, 359-362
[24] Stevenson, T. 1842. On the defects of raingauges with description of an improved form. Edin. New Phil. J., 33(65), 12-21
[25] Jevons, W.S. 1861. On the deficiency of rain in an elevated raingauge as caused by wind. London, Edinburgh & Dublin, Phil. Mag., Ser. 4, (22), 421-433
[26] Koschmieder, H. 1934. Methods and results of definite rain measurement. III. Danzig report. U.S.W.B. Mon. Weather Rev. 62: 5-7, illust.
[27] Brooks, C.F. 1938. Wind shields for precipitation gages. Trans. Amer. Geophys. Union, pp. 539-542, illust.
[28] Riesbol, H.H. 1938. Results from experimental rain gages at Coshocton, Ohio. Trans. AGU, pp. 542-550
[29] Warnick, C.C. 1953. Experiments with windshields for precipitation gages. Trans. AGU 34(3), 379-388
[30] Robinson, A.C., Rodda, J.C. 1969. Wind and the aerodynamic characteristics of raingauges, Meteorol. Mag. 98(1161), 113-120
[31] Sevruk, B. 1982. Methods of correction for systematic error in point precipitation measurement for operational use. World Meteorological Organizaton, Operational Hydrology, Report No. 21, WMO-No. 589
[32] Nespor, V., Sevruk, B. 1999. Estimation of wind-induced error of rainfall gauge measurements using a numerical simulation. J. Atmos. Ocean. Tech. 16, 450-464
[33] Habib, E., Krajewski, W.F. 2001. An example of computational approach used for aerodynamic design of a rain disdrometer. J. Hydraul. Res. 39(4), 425-428
[34] Van Heerden, W.M. 1964. Splash erosion as affected by the angle of incidence of raindrop impact. Ph.D. thesis, Purdue University, Lafayette, Ind. USA
[35] Lyles, L., Disrud, L.A., Woodruff, N.P. 1969. Effects of soil physical properties, rainfall characteristics, and wind velocity on clod disintegration by simulated rainfall. Soil Science Society of America Proc. 33, 302-306
[36] Lyles, L., Dickerson, J.D., Schmeidler, N.F. 1974. Soil detachment from clods by rainfall : effects of wind, mulch cover, and initial soil moisture. Trans. ASAE 17, 697-700
[37] Disrud, L.A. 1970. Magnitude, probability, and effect on kinetic energy of winds associated with rain in Kansas. Transactions Kans. Acad. Sci. 73(2), 237-246
[38] Disrud, L.A., Krauss, R.K. 1971. Examining the process of soil detachment from clods exposed to wind-driven simulated rainfall. Trans. ASAE 14, 90-92
[39] Moeyersons, J., De Ploey, J. 1976. Quantitative data on splash erosion, simulated on unvegetated slopes. Z. Geomorph. 25, 120-131
[40] Lyles, L. 1977. Soil detachment and aggregate disintegration by wind-driven rain. SCSA Special Publ. 21, 152-159
[41] Lal, R., Lawson, T.L., Anastase, A.H. 1980. Erosivity of tropical rains. In: De Boodt, M. and Gabriels, D. (editors), Assessment of erosion. Wiley, Chichester, pp. 143-151
[42] Jungerius, P.D., Verheggen, A.J.T., Wiggers, A.J. 1981. The development of blowouts in De Blink, a coastal dune area near Noordwijkerout, The Netherlands. Earth Surf. Proc. Land. 6, 375-396
[43] Moeyersons, J. 1981. S.T.O.R.M.-1 : a device for the simulation of oblique rain. First applications. – Geo-Eco-Trop 5, 163-180
[44] Moeyersons, J. 1983. Measurements of splash-saltation fluxes under oblique rain. Catena Suppl. 4, 19-31
[45] Poesen, J. 1985. An improved splash transport model. Z. Geomorph. N.F., 29, 2, 193-211

[46] De Lima, J.L.M.P. 1989. Raindrop splash anisotropy : slope, wind and overland flow velocity effects. Soil Technol. 2, 71-78
[47] Jungerius, P.D., Dekker, L.W. 1990. Water erosion in the dunes. Catena Suppl. 18, 185-193
[48] De Lima, J.L.M.P., Van Dijk, P.M., Spaan, W.P. 1992. Splash-saltation transport under wind-driven rain. Soil Technol., vol. 5, pp. 151-166
[49] Van Dijk, P.M., Stroosnijder, L., De Lima, J.L.M.P. 1996. The influence of rainfall on transport of beach sand by wind. Earth Surf. Proc. Land. 21, 341-352
[50] Gabriels, D., Tack, K., Erpul, G., Cornelis, W.M., Norton, L.D., Biesemans, J. 1997. Effect of wind-driven rain on splash detachment and transport of a silt loam soil: a short slope wind tunnel experiment. Workshop on Wind and Water Erosion, November 17-18 1997, Ghent, Belgium, pp. 87-93
[51] Goossens, D., Poesen, J., Gross, J., Spaan, W. 2000. Splash drift on light sandy soils: a field experiment. Agronomie 20, 271-282
[52] Erpul, G. 2001. Detachment and sediment transport from interril areas under wind-driven rain. Ph.D. thesis, Purdue University, 171p.
[53] Herwitz, S.R., Slye, R.E. 1995. Three-dimensional modeling of canopy tree interception of wind-driven rainfall. J. Hydrol. 168, 205-226
[54] Phillips, J.F.V. 1926. Rainfall interception by plants. Nature, December 11, 837-838
[55] Phillips, J.F.V. 1928. Rainfall interception by plants. Nature, March 10, 354-355
[56] McManus, P., Jones, A. 1994. Role of wind-driven rain, aerosols, and contaminated budwood in incidence and spatial pattern of fire blight in an apple nursery. Plant Dis. 11, 1059-1066
[57] Sache, I. 2000. Short-distance dispersal of wheat rust spores by wind and rain. Agronomie 20, 757-767
[58] Eldridge, H.J. 1976. Common defects in buildings. HMSO, pp. 486
[59] Lacasse, M.A., Vanier, D.J. (Editors) 1999a. Durability of building materials and components 8: Service life and asset management, Volume One: Service life and durability of materials and components. NRC Research Press, Ottawa, Canada, 898 p
[60] Lacasse, M.A., Vanier, D.J. (Editors) 1999b. Durability of building materials and components 8: Service life and asset management, Volume Two: Durability of Building assemblies and methods of service life prediction. NRC Research Press, Ottawa, Canada, 661 p
[61] Day, A.G., Lacy, R.E., Skeen, J.W. 1955. Rain penetration through walls. A summary of the investigations made at the UK Building Research Station from 1925 to 1955. Building Research Station Note. No. C.364 (unpublished)
[62] Garden, G.K. 1963. Rain penetration and its control. Canadian Building Digest, Division of Building Research, National Research Council, CBD40, pp. 401-404
[63] Freeman, I.L. 1975. Building failure patterns and their implications. The Architects' Journal, Vol. 161, No. 6, February 1975, pp. 303-308
[64] Reygaerts, J., Gasper, M., Dutordoir, C. 1976. 1200 problèmes. Erreurs de conception. Défauts de construction. Dégâts. (in French). Brussels, C.S.T.C. - revue, n° 3, September 1976
[65] Reygaerts, J., Gasper, M., Dutordoir, C., Leblanc, V. 1978. Comment éviter les dégâts (in French). Brussels, C.S.T.C. - revue, n° 3, September 1978
[66] Lacy, R.E. 1977. Climate and building in Britain. Her Majesty's Stationery Office, London
[67] Marsh, P. 1977. Air and rain penetration of buildings. The Construction Press Ltd., Lancaster, England. 174 p
[68] Whiteside, D., Newman, A.J., Kloss, P.B., Willis, W. 1980. Full-scale testing of the resistance to water penetration of seven cavity fills. Build. Environ., Vol. 15, pp. 109-118
[69] Newman, A.J., Whiteside, D., Kloss, P.B., Willis, W. 1982a. Full-scale water penetration tests on twelve cavity fills - Part I. Nine retrofit fills. Build. Environ., 17(3), 175-191
[70] Newman, A.J., Whiteside, D., Kloss, P.B. 1982b. Full-scale water penetration tests on twelve cavity fills - Part II. Three built-in fills. Build. Environ. 17(3), 193-207
[71] Rousseau, J. 1983. Rain penetration and moisture damage in residential construction. Building Science Insight '83, Seminar on Humidity, Condensation and Ventilation in Houses, Canada
[72] Pountney, M.T., Maxwell, R., Butler, A.J. 1988. Rain penetration of cavity walls: report of a survey of properties in England and Wales. Building Research Establishment Information Paper 2/88
[73] Price, C.A. 1975. The decay and preservation of natural building stone. Chemistry in Britain, 11, 10, (October 1975), 350-353
[74] Stupart, A.W. 1989. A survey of literature relating to frost damage in bricks. Masonry International 3(2), 42-50
[75] Maurenbrecher, A.H.P., Suter, G.T. 1993. Frost damage to clay brick in a loadbearing masonry building. Can. J. Civil Eng., 20, 247-253

[76] Franke, L., Schumann, I., van Hees, R., van der Klugt, L., Naldini, S., Binda, L., Baronio, G., Van Balen, K., Mateus, J. 1998. Damage atlas: classification and analyses of damage patterns found in brick masrony. European Commission Research report N° 8, vol. 2, Fraunhofer IRB Verlag
[77] Charola, A.E., Lazzarini, L. 1986. Deterioration of brick masonry caused by acid rain. ACS Symp. Series 318, 250-258
[78] White, R.B. 1967. The changing appearance of buildings. HMSO, London, 64 p
[79] Robinson, G., Baker, M.C. 1975. Wind-driven rain and buildings. Technical paper No. 445, Division of Building Research, National Research Council, Ottawa, Canada
[80] Baker, M.C. 1977. Rain deposit, water migration and dirt marking of buildings. RILEM/ASTM/CIB Symp. on Evaluation of the Performance of External Vertical Surfaces of Buildings. Otaniemi, Espoo, Finland. August 28-31 and September 1-2, 1977, Vol. 1, pp. 57-66
[81] El-Shimi, M., White, R., Fazio, P. 1980. Influence of facade geometry on weathering. Can. J. Civil Eng., Vol. 7, No. 4, pp. 597-613
[82] Huberty, J.M., De Smet, R. 1980. Duurzaamheid van het uitzicht van dagvlakbeton. Het verouderen van gevels (in Dutch). Brochure WTCB-FeBe-VCN
[83] Camuffo, D., Del Monte, M., Sabbioni, C., Vittori, O. 1982. Wetting, deterioration and visual features of stone surfaces in an urban area. Atmospheric Environment 16 (9), 2253-2259
[84] Verhoef, L.G.W. (editor) 1988. Soiling and cleaning of building facades. Report of the Technical Committee 62 Soiling and Cleaning of Building Facades (SCF) RILEM. Chapman and Hall, London
[85] Camuffo, D. 1992. Acid rain and deterioration of monuments: how old is the phenomenon? Atmospheric Environment, Vol. 26B, No. 2, pp. 241-247
[86] Verhoef, L.G.W., Cuperus, Y.J. 1993. Detailleren met baksteen. Voorkomen van visuele schade door vervuiling (in Dutch). Rapport 93-2 Civieltechnisch Centrum Uitvoering Research en Regelgeving – Koninklijk Verbond van Nederlandse Baksteenfabrikanten
[87] Etyemezian, V., Davidson, C.I., Zufall, M., Dai, W., Finger, S., Striegel, M. 2000. Impingement of rain drops on a tall building. Atmos. Environ., 34, 2399-2412
[88] Davidson, C.I., Tang, W., Finger, S., Etyemezian, V., Striegel, M.F., Sherwood, S.I. 2000. Soiling patterns on a tall limestone buildings: changes over 60 years. Environ. Sci. Technol., 34(4), 560-565
[89] Desadeleer, W. 2002. Invloed van detaillering of slagregengeïnduceerde pathologie van gebouwen : studie van cases en simulatie (in Dutch). MSc thesis, Laboratory of Building Physics, Katholieke Universiteit Leuven (unpublished)
[90] Blocken, B., Desadeleer, W., Carmeliet, J. 2002. Wind, rain and the building envelope: studies at the Laboratory of Building Physics, KULeuven. Proc. 6th Symp. on Building Physics in the Nordic Countries. Trondheim, Norway, June 17-19 2002, pp. 579-586
[91] New Builder. 1991. 17 January
[92] CWCT 1994. Facade engineering - a research survey, Centre for Window and Cladding Technology, University of Bath, UK
[93] Birkeland, O. 1965. General report. Rain penetration. RILEM/CIB Symp. on Moisture Problems in Buildings, Rain Penetration, Helsinki, August 16-19, Vol. 3, paper 3-0
[94] Bottema, M. 1993. Wind climate and urban geometry, Ph.D. thesis. FAGO. Technical University of Eindhoven
[95] Choi, E.C.C. 1993. Simulation of wind-driven-rain around a building. J. Wind Eng. Ind. Aerodyn. 46&47, 721-729
[96] Choi, E.C.C. 1994a. Determination of wind-driven-rain intensity on building faces. J. Wind Eng. Ind. Aerodyn. 51, 55-69
[97] Choi, E.C.C. 1994b. Parameters affecting the intensity of wind-driven rain on the front face of a building. J. Wind Eng. Ind. Aerodyn. 53, 1-17
[98] Choi, E.C.C. 1997. Numerical modeling of gust effect on wind-driven rain. J. Wind Eng. Ind. Aerodyn. 72, 107-116
[99] Choi, E.C.C. 1999b. Wind-driven rain on building faces and the driving-rain index. J. Wind Eng. Ind. Aerodyn. 79, 105-122
[100] Wisse, J.A. 1994. Driving rain, a numerical study. Proc. of 9th Symp. on Building Physics and Building Climatology, Dresden, 14-16 September 1994
[101] Karagiozis, A., Hadjisophocleous, G. 1996a. Wind-driven rain on high-rise buildings. Proc. of Thermal Performance of the Exterior Envelopes of Buildings VI – Moisture II, Clearwater, Florida, 399-405
[102] Karagiozis, A., Hadjisophocleous, G. 1996b. Wind-driven rain on tall buildings. Proc. of 4th Symp. of Building Physics in the Nordic Countries: Building Physics '96, Espoo, VTT Building Technology, 9-10 September 1996, 523-532
[103] Karagiozis, A., Hadjisophocleous, G., Cao, S. 1997. Wind-driven rain distributions on two buildings. J. Wind Eng. Ind. Aerodyn. 67&68, 559-572

[104] Van Mook, F.J.R. 1999a. Full-scale measurements and numeric simulations of driving rain on a building. 10ICWE, Copenhagen, Denmark, 21-24 June, 1145-1152
[105] Van Mook, F.J.R. 1999b. Measurements and simulations of driving rain on the Main Building of the TUE. 5th Symp. on Building Physics in the Nordic Countries, Göteborg, Sweden, 24-26 August, 377-384
[106] Van Mook, F.J.R. 2002. Driving rain on building envelopes. Ph.D. thesis. Building Physics Group (FAGO), Eindhoven University of Technology, Eindhoven University Press, Eindhoven, The Netherlands, 198 p
[107] Hagentoft, C.-E. 2001. Prediction of driving rain intensities using potential flows. Department of Building Physics, Chalmers University of Technology, Report R-01:4
[108] Hagentoft, C.-E., Högberg, A. 2002. Prediction of driving rain intensities using potential flows. Proc. 6th Symp. on Build. Phys. in the Nordic Countries. Trondheim, Norway, June 17-19, 2002, pp. 571-578
[109] Högberg, A. 2002. Microclimate load: transformed weather observations for use in design of durable buildings. Ph.D. thesis, Department of Building Physics, Chalmers University of Technology, Göteborg, Sweden, 162 p.
[110] Brown, B.L., 1988. Field measurements to gauge catch ratios of free-space driving rain on house walls at exposed estates in Dorset. Building Research Establishment Note, n. 127/88
[111] Van Mook, F.J.R., De Wit, M.H., Wisse, J.A. 1997. Computer simulation of driving rain on building envelopes. 2EACWE, Genova, Italy, 1997, 1059-1066
[112] Straube, J.F., Burnett, E.F.P. 1997a. Driving rain and masonry veneer. ASTM Symp. on Water Leakage Through Building Facades, Orlando, March 17 1996. Special Technical Publication, ASTM STP 1314, Philadelphia, 1997, 73-87
[113] Straube, J.F., Burnett, E.F.P. 2000. Simplified prediction of driving rain on buildings. Proc. of the International Building Physics Conf., Eindhoven, The Netherlands, 18-21 September 2000, 375-382
[114] Middleton, W.K. 1969. Invention of the meteorological instruments. The John Hopkins Press, Baltimore, Maryland
[115] Annals of Philisophy. 1816. Vol. 7, pp. 387-388
[116] Knox, T. 1837. Phil. Mag., Vol. 11, p. 260
[117] Phillips. 1840. B.A.A.S. Glasgow, Sections, pp. 45-47
[118] Chrimes, R. 1872. British rainfall (G.J. Symons), p. 31
[119] Beckett, H.E. 1938. Building Research Note, No. 755
[120] Lacy, R.E. 1951b. Observations with a directional raingauge. Q. J. Roy. Meteor. Soc. 77 (332), 283-292
[121] Holmgren, J. 1946. Klimaets innflytelse pa materialer og byggemate. Husbygging, 1, pp. 119-128. Oslo
[122] Holmgren, J., Landmark O., Vesterlid, A (Editors). 1949. Husbygging. B.1. Oslo
[123] Hoppestad, S. 1951. Studier over slagregnforhold. Mimeo. Intra-office report, Norwegian Building Research Institute, Oslo
[124] Hoppestad, S. 1955. Slagregn i Norge (in Norwegian). Norwegian Building Research Institute, rapport Nr. 13, Oslo
[125] Svendsen, S.D. 1955. Driving rain. Experimental research on the resistance of external walls against rain penetration. Norwegian Building Research Institute, Report No. 20, Oslo 1955
[126] Korsgaard, V., Madsen, T.L. 1962a. Apparatus for measuring and registering of driving rain. The Heat Insulation Laboratory, Technical University of Denmark, Copenhagen
[127] Korsgaard, V., Madsen, T.L. 1962b. Correlation between measured driving rain and computed driving rain. The Heat Insulation Laboratory, Technical University of Denmark, Copenhagen
[128] Korsgaard, V., Madsen, T.L. 1964a. A note on driving rain measurements. The Heat Insulation Laboratory, Technical University of Denmark, Copenhagen
[129] Korsgaard, V., Madsen, T.L. 1964b. Isoleringsevnen af nogle typiske ydervaegge udsat for det naturlige klima (in Danish). (The thermal insulation of some typical Danish outer walls exposed to the natural climate). The Heat Insulation Laboratory, Technical University of Denmark, Copenhagen
[130] Choi, E.C.C. 1996. Measurement of wind-driven rain. Proceedings of the 5th Australian Wind Engineering Society Workshop. Adelaide, 1996, paper A-6.
[131] Choi, E.C.C. 1999a. Characteristics of wind and wind-driven rain during tropical thunderstorms. Proc. of the 10th ICWE, Copenhagen, Denmark, 21-24 June 1999, 729-736
[132] Choi, E.C.C. 2001. Wind-driven rain and driving rain coefficient during thunderstorms and non-thunderstorms. J. Wind Eng. Ind. Aerodyn. 89, 293-308.
[133] Croiset, M. 1957. L'humidité des murs d'habitation. Etude des facteurs réels déterminant cette humidité et recherche de méthodes d'essais en oeuvre (in French). CSTB, Cahier 237, 27-54
[134] Birkeland, O. 1963. Rain penetration investigations. A summary of the findings of CIB Working Commission on Rain Penetration. Norwegian Building Research Institute, Rapport 36, Oslo
[135] Lacy, R.E. 1958. Directional raingauge observations at Thorntonhall, 1951-1955. Building Research Station Note B.181, Garston

[136] Lacy, R.E. 1964a. A note on driving rain at Garston. Building Research Station, Note No. EN 35
[137] Lacy, R.E. 1964b. Driving rain at Garston, United Kingdom. CIB Bulletin 4, pp. 6-9
[138] Lacy, R.E. 1965. Driving-rain maps and the onslaught of rain on buildings. RILEM/CIB Symp. on Moisture Problems in Buildings, Rain Penetration, Helsinki, August 16-19, Vol. 3, paper 3-4
[139] Couper, R.R. 1972. Drainage from vertical faces. Symp. on Wind-driven rain and the multi-storey building, Division of Building Research, CSIRO, paper 4
[140] Couper, R.R. 1974. Factors affecting the production of surface runoff from wind-driven rain. 2nd International CIB/RILEM Symp. on Moisture Problems in Buildings. Rotterdam, The Netherlands, September 10-12, 1974, paper 1.1.1
[141] Sankaran, R., Paterson, D.A. 1995a. Wind-driven rain: data collection facility at CSIRO, Sydney, Australia. 9ICWE, 1995, New Delhi, India, 2023-2033
[142] Sankaran, R., Roberts, G.F. 1999. Use of weather data in water resistant design of buildings. Proc. of the 10th ICWE, Copenhagen, Denmark, 21-24 June 1999, 1165-1170
[143] Bollen, S., Eerdekens, G. 1998. Regenbelasting van gevels. MSc thesis, Laboratory of Building Physics, Katholieke Universiteit Leuven, Leuven, Belgium, 215p
[144] Ritchie, T., Davison, J.I. 1969. The wetting of walls by rain. Internal report No. 367, Division of Building Research, National Research Council, Ottawa, Canada
[145] Straube, J., Schumacher, C., Burnett, E. 1995. In-service performance of enclosure walls: construction and instrumentation report. Report N2L 3G1 BEG Building Engineering Group, University of Waterloo, Waterloo, Ontario, Canada
[146] Straube, J.F., Burnett, E.F.P. 1997b. Rain control and screened wall systems. Proc. 7th Conf. on Building Science and Technology. Durability of Buildings. Design, Maintenance, Codes and Practices. Toronto, 20-21 March 1997
[147] Straube, J.F. 1998. Moisture control and enclosure wall systems. Ph.D Thesis. University of Waterloo, Ontario, Canada
[148] Jessing, Y. 1959. Statistical treatment of data on driving rain. Danish National Institute of Building Research, Note B-42(3)/F-162 (unpublished)
[149] Flori, J.P. 1990. Mouillage et sechage d'une façade verticale – analyse experimentale (in French). EN-CLI 90.2 L, CSTB, Nantes (unpublished)
[150] Flori, J.P. 1991. Mouillage et sechage d'une façade en brique – analyse experimentale (in French). EN-CLI 91.3 L, CSTB, Nantes (unpublished)
[151] Flori, J.P. 1992. Influence des conditions climatiques sur le mouillage et le séchage d'une façade verticale (in French). Cahiers du CSTB, livraison 332, September 1992, cahier 2606
[152] Künzel, H. 1976. Beurteilung der Schlagregenbeanspruchung und des Regenschutzes von Gebäuden. IBP-Bericht B.Ho 5/76
[153] Künzel, H.M. 1993. Rain loads on building elements. Contribution to the IEA-Annex-24 meeting, Report T2-D-93/02, Holzkirchen, October 1993
[154] Künzel, H., Schwarz, B. 1968. Die Feuchtigkeitsaufnahme von Baustoffen bei Beregnung. Berichte aus der Bauforschung, Heft 51, pp. 99-113, W. Ernst und Sohn, Berlin
[155] Schwarz, B. 1973b. Die Schlagregenbeanspruchung von Gebäuden. Messmethoden – Messgeräte (in German). In: Schlagregen. Messmethoden – Beanspruchung – Auswirkung. Institut für Bauphysik der Fraunhofer-Gesellschaft, Berlin 1973
[156] Frank, W., Schwarz, B., Künzel, H., Gosele, K. 1977. Schlagregen, Wandfeuchtigkeit, Wärmeverbrauch. Institut für technische Physik, Stuttgart B.Ho.
[157] Isaksen, T. 1965. Rain penetration joints. Influence of dimensions and shape of joint on rain penetration. RILEM/CIB Symp. on Moisture Problems in Buildings, Rain Penetration, Helsinki, August 16-19, 1965, Vol. 3, paper 3-5
[158] Isaksen, T. 1975. Driving rain in Bergen. Norwegian Building Research Institute F4625, Trondheim
[159] Henriques, F.M.A. 1992. Quantification of wind-driven rain – an experimental approach. Building Research and Information 20(5), 295-297
[160] Varnbo, B. 1966. Slagregn. Svenska Riksbyggen. Handling nr 14. Stockholm
[161] Järnmark, T. 1968. Slagregn. (Statens Institut för Byggnadsforskning). Informationsblad 39 :1968 och 40:1968. Stockholm.
[162] Beijer, O.F. 1976. Driving rain against external walls of concrete. Swedish Cement and Concrete Research Institute. Research 7:76. Stockholm 1976, 92p
[163] Beijer, O. 1977. Concrete walls and weathering. RILEM/ASTM/CIB Symp. on Evaluation of the Performance of External Vertical Surfaces of Buildings. Otaniemi, Espoo, Finland. August 28-31 and September 1-2, 1977, Vol. 1, pp. 67-76

[164] Jacobson, L. 1977. Driving rain in vertical surfaces at CTH field station for building research and testing. RILEM/ASTM/CIB Symp. on Evaluation of the Performance of External Vertical Surfaces of Buildings. Otaniemi, Espoo, Finland. August 28-31 and September 1-2, 1977, Vol. 1, pp. 170-180
[165] Newman, A.J. 1987. Microclimate and its effects on durability. Chemistry and Industry 17, 583-593
[166] Basart, A. 1946. Verhandeling inzake de regenval op het verticale vlak met betrekking tot de bouwconstructie. Technical Report (In Dutch), Instituut voor warmte-economie TNO. Keramisch Instituut TNO
[167] Hendry, I.W.L. 1964. Comparison between two types of wall rain gauge. Building Rsearch Station, Internal note, SL/IN.1.
[168] Meert, E., Van Ackere, G. 1977. Dichtheid van gevels en daken (in Dutch). Wetenschappelijk en Technisch Centrum voor het Bouwbedrijf, eindverslag, Brussel
[169] Meert, E., Van Ackere, G. 1978. L'Etancheité au vent et à la pluie des facades (in French). C.S.T.C. revue, No. 2(3), June 1978
[170] Ali Mohamed, F., Hens, H. 1992. Outdoor climate, reference year, driving rain, T2-B-92/05 (unpublished)
[171] Hens, H., Ali Mohamed, F. 1994. Preliminary results on driving rain estimation. Contribution to the IEA annex 24, Task 2 – Environmental conditions, T2-B-94/02
[172] Blocken, B., Carmeliet, J. 2000a. Driving rain on building envelopes – I: numerical estimation and full-scale experimental verification. J. Thermal Env. & Bldg. Sci., July, 24(1), 61-85
[173] Blocken, B., Carmeliet, J. 2000b. Driving rain on building envelopes – II: representative experimental data for driving rain estimation. J. Thermal Env. & Bldg. Sci., October, 24(2), 89-110
[174] Blocken, B., Carmeliet, J. 2002. Spatial and temporal distribution of driving rain on a low-rise building. Wind Struct. 5(5), 441-462
[175] Blocken, B., Van Mook, F., Hagentoft, C.-E., Carmeliet, J. 2001. A status report of numerical-experimental driving rain studies on 3 full-scale buildings. 3rd EACWE, 2-6 July 2001, Eindhoven, The Netherlands, pp. 133-140
[176] Kragh, M.K. 1998. Microclimatic conditions at the external surface of building envelopes. Ph.D thesis, Department of Buildings and Energy, Technical University of Denmark
[177] Hilaire J. and Savina, H. 1988. Pluie battante sur une facade d'immeuble (in French). EN-CLI 88.5 R, CSTB, Nantes
[178] Künzel, H. 1970. Schlagregenschutz von Gebäuden. Im Jahrbuch der Fraunhofer-Gesellschaft München, 70/71, pp.. 97-104
[179] Künzel, H. 1986. Der Regenschutz von Aussenwänden (in German). Mauerwerk-Kalender 1986, 735-751
[180] Künzel, H., Frank, W., Schwarz, B. 1971. Schlagregen – Wandfeuchtigkeit – Wärmeverbrauch, Bericht an das Bundesministerium für Städtebau u. Wohnungswesen. B. Ho 10/71
[181] Helbig, A. 1972. Messungen der Schlagregen Intensität am Gebäude. Abh. Des Meteorologischen Dienstes der DDR, Nr. 105
[182] Schwarz, B. 1973a. Witterungsbeanspruchung von Hochhausfassaden (in German). HLH (Heizung, Lüftung/Klimatechnik, Haustechnik), Bd. 24, Nr. 12, 376-384
[183] Frank, W. 1973. Einwirkung von Regen und Wind auf Gebäudefassaden. Stand der gegenwärtigen Kenntnisse aufgrund der Literatur (in German). In: Schlagregen. Messmethoden – Beanspruchung – Auswirkung. Institut für Bauphysik der Fraunhofer-Gesellschaft, Berlin 1973
[184] Scultetus, H.R. 1974. Sechsjährige Schlagregenmessungen in Braunschweig-Völkenrode. (in German) Landbauforschung Völkenrode, 24, 2, 149-158
[185] Lammel, G., Metzig, G. 1997. Pollutant fluxes onto the facades of a historical monument. Atmos. Environ. 31 (15) : 2249-2259
[186] Kerr, D., Freathy, P.E. 1998. To develop a European standard dynamic watertightness test for curtain walling. Proc. of the 4th UK Conf. on Wind Engineering, Bristol, 2-4 September 1998, 35-40
[187] Ishizaki, H., Mitsuta, Y., Sano, Y. 1970. Rainfall deposit on a wall of a building in a storm. Bulletin of the Disaster Prevention Research Institute, Kyoto University, 20(2), No. 174, (December 1970), 95-103
[188] Ito, H. et al. 1983. Measurement of driving rain on external wall of a building (in Japanese). Proc. of the Annual Meeting of the Architectural Institute of Japan
[189] Ishikawa, H. 1988. Driving rain impaction on a high-rise building. Proc. Faculty of Engineering, Tokyo University, Japan, Vol. 14, 1-21
[190] Van Mook, F.J.R. 1996. A plan for the measurement of driving rain on a building. 3rd BEATRICE EuroConf., Nantes, 4-6 September 1996
[191] Van Mook, F.J.R. 1998a. Description of the measurement set-up for wind and driving rain at the TUE. Report FAGO 98.04.K
[192] Van Mook, F.J.R. 1998b. Measurements of driving rain by a new gauge with a wiper. Report FAGO 98-62.K

[193] Högberg, A.B., Kragh, M.K., van Mook, F.J.R. 1999. A comparison of driving rain measurements with different gauges. Proc. of the 5th Symp. Build. Phys. in the Nordic Countries, Gothenburg, 24-26 August 1999, 361-368
[194] Ryd, H. 1970. Research in building climatology with special reference to the problem of snow and rain in connection with wind. CIB-Symp. Climatology and Building, Vienna
[195] Holmgren, O. 1972. Snow loads, driving rain and building design. Colloquium Teaching the Teachers on Building Climatology. Statens Institut for Byggnadsforskning, Stockholm. Preprint No. 35
[196] Sandin, K. 1973. Fukt- och temperaturundersökning I Vadstena Klosterkyrka. Inst. for byggnadsteknik, Tekniska Högskolan i Lund. Rapport 50
[197] Sandin, K. 1980. The effect of the rendering on the moisture balance of the facade – main report (in Swedish). Rapport TVBM – 1004. Division of Building Materials, Lund Institute of Technology, Sweden
[198] Sandin, K. 1984. The effect of moisture on the energy flow through outer walls (in Swedish). Rapport TVBM – 3019. Division of Building Materials, Lund Institute of Technology, Sweden
[199] Sandin, K. 1987. The moisture condition in aerated lightweight concrete walls. In situ measurements of the effect of the driving rain and the surface coating. Rapport TVBM – 3026. Division of Building Materials, Lund Institute of Technology, Sweden
[200] Sandin, K. 1991. Skalmurskonstruktionens fukt- och temperaturbetingelser. Rapport R43: 1991 Byggforskningsradet, Stockholm, Sweden
[201] Sandin, K. 1994. Moisture conditions in cavity walls with wooden framework. Building Research and Information 21, pp. 235-238
[202] Lyberg, M. 1979. Review of Micro- and Building Physical Properties of Driving Rain, Swedish Institute for Building Research, Bulletin M79:13E
[203] Lyberg, M. 1980. Results from driving rain measurements on a tall apartment building 1969-1978. Proc. of the CIB Working Group W61 Joints in Exterior Walls 1979, Danish Building Research Institute
[204] Högberg, A. 1998. Microclimate description: To facilitate estimating durability and service life of building components exposed to natural outdoor climate. Chalmers University of Technology, Publication P-98:5.
[205] Högberg, A. 1999a. Microclimate measurement focused on wind-driven rain striking building surfaces. Proc. of the 5th Symp. on Building Physics in the Nordic Countries, Gothenburg, 24-26 August 1999, 369-376
[206] Högberg, A. 1999b. Measurement of microclimate near a building surface. Proc. of the 10th International Symp. for Building Physics and Building Climatology, Dresden, Germany, September 27-29, 1999, pp. 649-657
[207] Adl-Zarrabi, B., Högberg, A. 2001. Microclimate: field measurements, driving rain analyses. Proc. of Performance of the Exterior Envelopes of Whole Buildings VIII: Integration of Building Envelopes, Florida, US, December 2-6, 2001
[208] Lacy, R.E. 1959. Driving-rain measurements in Scotland 1956-57. Building Research Station, Note B. 182 (unpublished)
[209] Harrison, H.W., Bonshor, R.B. 1970. Weatherproofing of joints: a systematic approach to design. Proc. of the Conf. on Joints in Structures held at the University of Sheffield, July 8-10, Session D, paper 3
[210] Cronshaw, J.L. 1971. Rainwater run-off from walls. London, Building. 12 February 1971. 7/123
[211] Herbert, M.R.M. 1974. Some observations on the behaviour of weather protective features on external walls. Building Research Establishment Current Paper, CP 81/74
[212] Prior, M.J., Newman, A.J. 1988. Driving rain - calculations and measurements for buildings. Weather, 43, 146-155
[213] Osmond, S.D. 1995. Assessment of the full scale micro climate around buildings. Building Research Establishment Note, N47/95 (unpublished)
[214] Osmond, S.D. 1996. Assessment of the full scale micro climate around buildings. Building Research Establishment Note, N91/96 (unpublished)
[215] Kerr, D., Matthews, R., Kirmayr, T. 1997. To develop a European standard dynamic watertightness test for curtain walling. Proc. of the 2nd EACWE, Genova, Italy, 22-26 June 1997, Vol. 2, 1051-1058
[216] Tsvid, A.A. 1960. The measurement of precipitation striking vertical surfaces. Meteorologiya i Gidrologiya, No. 11
[217] Mink, J.F. 1960. Distribution patterns of rainfall in the leeward Koolau Mountains, Oahu, Hawaii. J. Geophys. Res. 65(9), 2869-2876
[218] Camuffo, D. 1998. Microclimate for cultural heritage. Elsevier, Amsterdam
[219] Flower, J.W., Lawson, T.V. 1972. On the laboratory representation of rain impingement on buildings. Atmos. Environ., 6, 55-60
[220] Rayment, R., Hilton, M. 1977. The use of bubbles in a wind tunnel for flow-visualisation and the possible representation of raindrops. J. Ind. Aerodyn. 2, 149-157

[221] Surry, D., Inculet, D.R., Skerlj, P.F., Lin, J-X., Davenport, A.G. 1994a. Wind, rain and the building envelope: a status report of ongoing research at the University of Western Ontario. J. Wind Eng. Ind. Aerodyn., 53, 19-36
[222] Inculet, D., Surry, D. 1994. Simulation of wind-driven rain and wetting patterns on buildings. BLWTL-SS30-1994. Final report
[223] Inculet, D.R. 2001. The design of cladding against wind-driven rain. Ph.D. thesis, The University of Western Ontario, London, Canada, 297 p.
[224] Blocken, B., van Mook, F.J.R., Högberg, A. 1999. Full-scale driving rain simulation in the Jules Verne Climatic Wind Tunnel. Training and Mobility of Researchers, Access to Large-Scale Facilities – Access for researchers, Research proposal, 11p. Unpublished
[225] Gandemer, J. 2001. Final report: Large Scale Facilities, Jules Verne Climatic Wind Tunnel, Contract ERB 4062PL970118. Unpublished
[226] Lacy, R.E., Shellard, H.C. 1962. An index of driving rain. Meteorol. Mag. 91, 177-184
[227] Lacy, R.E. 1971. An index of exposure to driving rain. Building Research Station Digest 127, Garston 1971
[228] Jessing, J. 1966. An index of driving rain in Denmark. CIB Working Commission on Rain Penetration, Madrid
[229] Blociszewski, S. 1966. Driving rain in Poland. CIB Working Commission on Rain Penetration, Madrid
[230] Jonesen, C., Marcu, J. 1966. Some aspects on the rain penetration problem through the building walls in Rumania. CIB Working Commission on Rain Penetration, Madrid
[231] Avendano, P. 1966. Present state of EXCO's research on rain penetration of buildings. CIB Working Commission on Rain Penetration, Madrid
[232] Caspar, W. 1966. Schlagregen-Index-Karte fûr das Gebiet der Bundesrepublik Deutschland. (In German). CIB Working Commission on Rain Penetration, Madrid
[233] Künzel, H. 1966. Zur Frage der Beurteilung der Schlagregenbeanspruchung in einzelnen Gebieten und Ländern, Berichte an der Bundesministerium fûr Wohnungswesen und Städtebau
[234] Lacy, R.E. 1976. Driving-rain index. Building Research Establishment Report, Her Majesty's Stationery Office, London
[235] Prior, M.J. 1985. Directional driving rain indices for the United Kingdom - computation and mapping. Building Research Establishment Report, Garston
[236] British Standards Institution. 1984. Methods for assessing exposure to wind-driven rain. Draft for Development 93
[237] British Standards Institution. 1992. Code of practice for assessing exposure of walls to wind-driven rain – BS8104
[238] CEN 1997. Hygrothermal performance of buildings – Climatic data – Part 3: Calculation of a driving rain index for vertical surfaces from hourly wind and rain data. Draft prEN 13013-3
[239] Sanders, C. 1996. Heat, air and moisture transfer in insulated envelope parts, Final report – vol. 2, task 2: Environmental conditions. Acco, Leuven
[240] Boyd, D.W. 1963. Driving-rain map of Canada. Technical note No. 398, Division of Building Research, National Research Council, Ottawa, Canada
[241] Shver, T.A. 1971. On estimating the wetting of walls by driving rain. American Geographical Society - Soviet Geography: Review & Translation 12(10), 701-710
[242] Eichler, F. 1970a. Schlagregen und seine Auswirkungen (in German). Stadt- und Gebäudetechnik 6, 145-147
[243] Eichler, F. 1970b. Schlagregen und seine Auswirkungen (in German). Stadt- und Gebäudetechnik 7, 176-179
[244] Grimm, C.T. 1982. A driving rain index for masonry walls. Masonry: Materials, Properties and Performance, ASTM STP 778, Borchelt J.G. (Ed.) 171-177
[245] Underwood, S.J., Meentemeyer, V. 1998. Climatology of wind-driven rain for the contiguous United States for the period 1971 to 1995. Phys. Geogr. 19 (6), 445-462
[246] Sauer, P. 1987. An annual driven rain index for China. Build. Environ., 22, 4, 239-240
[247] Chand, I., Bhargava, P.K. 2002. Estimation of driving rain index for India. Build. Environ. 37, 549-554
[248] Laws, J.O., Parsons, D.A. 1943. Relation of raindrop size to intensity. Trans. AGU 24 (2), 453-460
[249] Best, A.C. 1950b. Empirical formulae for the terminal velocity of water drops falling through the atmosphere. Q. J. Roy. Meteor. Soc. 76, 302-311
[250] Best, A.C. 1950a. The size distribution of raindrops. Q. J. Roy. Meteor. Soc. 76, 16-36
[251] Künzel, H.M. 1994. Verfahren zur ein- und zweidimensionalen Berechnung des gekoppelten Wärme- und Feuchtetransports in Bauteilen mit einfachen Kennwerten. Ph.D thesis. Fakultät Bauingenieur- und Vermessungswesen. Universität Stuttgart

[252] Morris, S. 1975. A wall penetration map of Canada. Atmos. Environ. Service, Downsniew, Ontario, Canada
[253] Sneyers, R., Meert, E., Soubrier, D., Van Ackere, G. 1979. Intensité de la pluie battante et pression du vent sur les facades (in French). C.S.T.C. revue, No. 2(3), June 1979
[254] Choi, E.C.C. 1994c. Characteristics of the co-occurrence of wind and rain and the driving-rain index. J. Wind Eng. Ind. Aerodyn. 53, 49-62
[255] Fazio, P., Mallidi, S.R., Zhu, D. 1995. A Quantitative study for the measurement of driving rain exposure in the Montreal region. Build. Environ., 30, 1, 1-11
[256] Zhu, D., Mallidi, S.R., Fazio, P. 1995a. Approach for urban driving rain index by using climatological data recorded at suburban meteorological station. Build. Environ., 30, 2, 229-236
[257] Zhu, D., Mallidi, S.R., Fazio, P. 1995b. Quantitative driving rain exposure on a vertical wall at various Canadian cities. Build. Environ., 30, 4, 533-544
[258] Thein, W. 1933. Massgebliche schlagregenwirkungen in der Bautechnik (in German). Annalen der hydrographie und Maritimen Meteorologie, July 1933, 196-201
[259] Zobel, R.F. 1965. Wind strength and rainfall - are they related? Weather 20, 13-16
[260] Linforth, D.J. 1972. Meteorological data for Melbourne relating to wind-driven rain. Symp. on Wind-driven rain and the multi-storey building, Division of Building Research, CSIRO, paper 1
[261] Gordon, B. 1972. Meteorological data for Brisbane relating to wind-driven rain. Symp. on Wind-driven rain and the multi-storey building, Division of Building Research, CSIRO, paper 2
[262] Sacré, C. 1978. Etude corrélative de la pluie et du vent à la station climatologique du C.S.T.B (in French). Nantes. Rapport C.S.T.B. - EN - CLI 78.2 C (1978)
[263] Sacré, C. 1982. Concommitance de la pluie et du vent en France. Approche statistique (in French). Cahiers du CSTB, n° 232, September 1982, cahier 1792
[264] Sadagashvili, G.R., Kartvelishvili, L.G. 1982. Method of meteorological observation treatment for estimation driving rain parameters. Proc. of the Symp. on Building Climatology, Moscow, 1982, pp. 602-610
[265] Beguin, D. 1985. Etude pour la France du risque de mouillage par la pluie des parois verticales de la construction (in French). EN-CLI 85-82., CSTB, Nantes
[266] Murakami, S., Iwasa, Y., Morikawa, Y., Chino, N. 1987. Extreme wind speeds for various return periods during rainfall. J. Wind Eng. Ind. Aerodyn. 26, 105-125
[267] Choi, E.C.C. 1992. Extreme wind speeds during rainfall. Australian Wind Engineering Society 2nd Workshop, Melbourne, Australia
[268] Tsimplis, M.N. 1994. The correlation of wind speed and rain. Weather 49, 135-139
[269] Surry, D., Skerlj, P.F., Mikitiuk, M.J. 1994b. An exploratory study of the climatic relationships between rain and wind, interim report to CMHC for review, Boundary Layer Wind Tunnel Laboratory, University of Western Ontario
[270] Flori, J.P. 1995. Analyse de la concomitance pluie-vent (in French). EN-CLI 95.8 L, CSTB, Nantes (unpublished)
[271] Sandberg, P.I. 1974. Driving rain distribution over an infinitely long high building: computerized calculations. 2nd International CIB/RILEM Symp. on Moisture Problems in Buildings. Rotterdam, The Netherlands, 10-12 September 1974, Paper 1-1-2
[272] Rodgers, G.G., Poots, G., Page, J.K., Pickering, W.M. 1974a. Rain impaction on a slab type building: a theoretical approach. 2nd International CIB/RILEM Symp. on Moisture Problems in Buildings. Rotterdam, The Netherlands, 10-12 September 1974, Paper 1-1-3
[273] Rodgers, G.G., Poots, G., Page, J.K., Pickering, W.M. 1974b. Theoretical predictions of rain drop impaction on a slab type building. Build. Sci. 9, 181-190
[274] Rodgers, G.G. 1977. Theoretical studies of the interaction of wind flow with precipitation elements in determining the deposition of rain, snow and ice on buildings and structures. Sixth Course Airflow and Building Design. Sheffield University
[275] Souster, C. 1979. A theoretical approach to predicting snow loads and driving rain deposition on buildings. Ph.D. thesis, University of Sheffield, UK
[276] Choi, E.C.C. 1991. Numerical simulation of wind-driven-rain falling onto a 2-D building. Asia Pacific Conf. on Computational Mechanics, Hong Kong, pp. 1721-1728
[277] Choi, E.C.C. 1997. Velocity and impact direction of wind-driven rain on building faces. International Conference on Building Envelope Systems and Technology, Bath, UK, 1997, pp. 465-472.
[278] Choi, E.C.C. 2000. Variation of wind-driven rain intensity with building orientation. ASCE Journal of Architectural Engineering 6(4): 122-128.
[279] Bookelmann, J., Wisse, J. 1992. Numerical estimate of driving rain. Inaugural Conf. of the Wind Engineering Society, Cambridge, UK, 28-30 September 1992

[280] Sankaran, R., Paterson, D.A. 1995b. Computation of rain falling on a tall rectangular building. 9ICWE, 1995, New Delhi, India, 2127-2137
[281] Sankaran, R., Paterson, D.A. 1997. Computation of rain falling on a tall rectangular building. J. Wind Eng. Ind. Aerodyn. 72, 127-136
[282] Hangan, H. 1999. Wind-driven rain studies. A C-FD-E approach. J. Wind Eng. Ind. Aerodyn., 81, 323-331
[283] Lakehal, D., Mestayer, P.G., Edson, J.B., Anquetin, S., Sini, J.-F. 1995. Eulero-Lagrangian simulation of raindrop trajectories and impacts within the urban canopy. Atmos. Environ., 29, 23, 3501-3517
[284] Segersson, D. 2003. Numerical quantification of driving rain on buildings, Reports Meteorology and Climatology, No. 103, Swedish Meteorolgical and Hydrological Institute (SMHI).
[285] Ruegg, F. W., 1996. Storm-driven trajectories of rain near balconies on tall building. J. Arch. Eng. Sept. 1996, 100-106
[286] Choi, E.C.C. 2002. Modeling of wind-driven rain and its soil detachment effect on hill slopes. J. Wind Eng. Ind. Aerodyn. 90: 1081-1097.
[287] Versteeg, H.K., Malalasekera, W. 1995. An introduction to computational fluid dynamics, the finite volume method. Longman Scientific and Technical.
[288] Franke, J., Hirsch, C., Jensen, A.G., Krüs, H.W., Schatzmann, M., Westbury, P.S., Miles, S.D., Wisse, J.A., Wright, N.G. 2004. Recommendations on the use of CFD in wind engineering. Proceedings of the International Conference on Urban Wind Engineering and Building Aerodynamics, (Ed. van Beeck, J.P.A.J.), COST Action C14, Impact of Wind and Storm on City Life and Built Environment, von Karman Institute, Sint-Genesius-Rode, Belgium, 5-7 May 2004.
[289] Shih, T-H., Liou, W.W., Shabbir, A., Zhu, J. 1995. A new k-ε eddy-viscosity model for high Reynolds number turbulent flows – model development and validation. Comp. Fluids 24(3), 227-238
[290] Kim, S-E., Choudhury, D., Patel B. 1997. Computations of complex turbulent flows using the commercial code FLUENT. Proc. of the ICASE/LaRC/AFOSR Symp. on Modeling Complex Turbulent Flows, Hampton, Virginia
[291] Murakami, S., Mochida, A. 1988. 3-D numerical simulation of airflow around a cubic model by means of the k-ε model. J. Wind Eng. Ind. Aerodyn. 31: 283-303
[292] Baetke, F., Werner, H., Wengle, H. 1990. Numerical simulation of turbulent flow over surface-mounted obstacles with sharp edges and corners. J. Wind Eng. Ind. Aerodyn. 35: 129-147
[293] Baskaran, A., Stathopoulos, T. 1992. Influence of computational parameters on the evaluation of wind effects on the building envelope. Build. Environ. 27(1): 39-49
[294] Salles, C., Creutin, J-D., Sempere-Torres, D. 1998. The optical spectropluviometer revisited. J. Atmos. Ocean. Tech. 15, 1215-1222
[295] Salles, C., Poesen, J., Borselli, L. 1999. Technical communication. Measurement of simulated drop size distribution with an optical spectro pluviometer: sample size considerations. Earth Surf. Proc. Land. 24, 545-556
[296] Salles, C., Poesen, J. 1999. Performance of an optical spectro pluviometer in measuring basic rain erosivity characteristics. J. Hydrol. 218, 142-156
[297] Marshall, J.S., Palmer, W.M. 1948. The distribution of raindrops with size. J. Meteor. 5, (August), 165-166
[298] Mualem, Y., Assouline, S. 1986. Mathematical model for rain drop distribution and rainfall kinetic energy. Trans. ASAE 29(2), (March-April), 494-500
[299] Morsi, S.A., Alexander, A.J. 1972. An investigation of particle trajectories in two-phase flow systems. J. Fluid Mech. 55, 193-208
[300] Pruppacher, H., Klett, J. 1978. Microphysics of clouds and precipitation. D. Reidel, Boston
[301] Gunn, R., Kinzer, G.D. 1949. The terminal velocity of fall for water droplets in stagnant air. J. Meteor. 6, (August), 243-248
[302] Van der Hoven, I. 1957. Power spectrum of horizontal wind speed in the frequency range from 0.0007 to 900 cycles per hour. J. Meteor. 14, 160-164
[303] Fluent Inc. 1998. Fluent 5 User's Guide.

FIGURE CAPTIONS:

Fig. 1. Rain intensity vector **R** and its components: wind-driven rain intensity $\mathbf{R}_{wdr}$ and horizontal rainfall intensity $\mathbf{R}_h$

Fig. 2. A representation of the wind flow pattern around a building and of raindrop trajectories in the wind flow pattern. The flow pattern includes a frontal vortex (A), corner streams (B), separation at building corners (C), recirculation zones (D), shear layers (E) and a far wake (F) (figure partly from [94], ©Bottema 1993, reproduced with permission)

Fig. 3. Horizontal rainfall gauge with a horizontal aperture to measure horizontal rainfall (left) and wind-driven rain gauge with a vertical aperture to measure wind-driven rain (right) (from [125])

Fig. 4 (a) Free-standing wind-driven rain gauge designed at the Building Research Station, UK, in 1936, with eight vertical apertures and one horizontal aperture (©BRE 2003, reproduced with permission). (b) Free-standing wind-driven rain gauge designed at the Norwegian Building Research Institute in 1937, with four vertical apertures and one horizontal aperture (from [134])

Fig. 5. (a) Circular free-standing wind-driven rain gauge and (b) funnel-shaped free-standing wind-driven rain gauge designed at the TUD in the beginning of the 1960s (from [129], ©Korsgaard and Madsen 1964b, reproduced with permission)

Fig. 6. Wall-mounted plate-type wind-driven rain gauge where the collection area fits flush into the vertical facade surface

Fig. 7. Wall-mounted plate-type wind-driven rain gauge where the collection area is recessed in the wall (from [133])

Fig. 8. Photographs of wall-mounted plate-type wind-driven rain gauges: (a) two gauges with the collection area fitting flush into the wall surface placed side-by-side for comparison trials at the TNO Institute for Building Materials (left: TNO gauge, right: BRS gauge) (from [138], ©BRE 2003, reproduced with permission). (b) The recessed gauge designed by Croiset placed in a wall of the test house of the Heat Insulation Laboratory, TUD (from [129], ©Korsgaard and Madsen 1964b, reproduced with permission)

Fig. 9. Special wind-driven rain gauge designed to measure adhesion water. The collection plate and the reservoir are suspended from a load cell (figure partly from [106], ©van Mook 2002, reproduced with permission)

Fig. 10. Special wind-driven rain gauge designed to measure adhesion water. The collection area is equipped with an automated wiper (figure partly from [106], ©van Mook 2002, reproduced with permission)

Fig. 11. Simulation and measurement results of the performance of the KUL wind-driven rain gauge with 0.3x0.3 m² rectangular collection area made of PVC. The curve "adhered water" is an indication of the adhesion-water-evaporation error.

Fig. 12. Special wind-driven rain gauge designed to limit splashing losses. The collection area is deeply recessed and composed of tilted surfaces (figure partly from [109], ©Högberg 2002, reproduced with permission)

Fig. 13 (a) VLIET test building. North-west and south-west facade. Building dimensions, roof overhang length, positions and numbers (1-9) of wind-driven rain gauges type KUL. (b) Spatial distribution of measured catch ratio values at the end of the rain event given in Fig. 14a. Estimated measurement error: 0.04. Multiply catch ratio values with S_h = 24.8 mm to obtain the wind-driven rain amount.

Fig. 14 (a) Measurement values of wind speed U_i and horizontal rainfall intensity R_{hi} (left axis) and wind direction φ_i (right axis) for each 10-minute interval in the 5-day rain event (01-05/01/1998). Total horizontal rainfall amount S_h = 24.8 mm. The wind direction is approximately perpendicular to the south-west facade ($\varphi_i \approx$ 225°) (b) Temporal distribution of cumulative measured wind-driven rain amount during the rain event at gauge position 7

Fig. 15. Wind-driven rain maps of the United Kingdom (from [227], ©BRE 2003, reproduced with permission). Left: omnidirectional wind-driven rain map with exposure grading (white = sheltered, light gray = moderate, dark gray = severe). Right: directional wind-driven rain map where the length of the petals indicates the magnitude of the wind-driven rain index from different directions

Fig. 16. Wall factors as provided by the European Standard Draft to take into account the type of wall (height, roof overhang) and the variation of the WDR across the surface of the wall (CEN 1997, [238], ©CEN 2004, reproduced with permission)

Fig. 17. Wind flow pattern around a building (10x10x40 m^3) calculated with CFD. (a) Longitudinal flow in the centerplane of the building. (b) Flow in a horizontal plane at midheight of the building (from [96], ©Elsevier 2004, reproduced with permission).

Fig. 18. Perspective, side and plan view of raindrop trajectories for (a) 5 mm radius raindrops and (b) 0.25 mm radius raindrops both in the 10 m/s flow field (from [96], ©Elsevier 2004, reproduced with permission).

Fig. 19. Configuration of the building modeled by Choi [96] and division into 12 large areas on the windward facade of the building.

Fig. 20. Spatial distribution of calculated catch ratio values at the end of the rain event that is illustrated in Fig. 14a. Wind direction is perpendicular to the south-west facade. Contour lines and maximum values for each module are given. Areas sheltered from rain are colored black. The calculated values at the wind-driven rain gauge positions are additionally indicated for comparison with the corresponding measurements in Fig. 13b.

Fig. 21. Temporal distribution of experimentally and numerically determined wind-driven rain amount during the rain event at gauge position 7

Table 1
Countries where field measurements of free wind-driven rain have been/are being conducted for use in building research (in alphabetical order)

Country	Author(s) and date of publication	References
Australia	Couper (1972)*, Couper (1974), Sankaran and Paterson (1995a), Sankaran and Roberts (1999)	[139-142]
Belgium	Bollen and Eerdekens (1998)	[143]
Canada	Ritchie and Davison (1969), Straube et al. (1995), Straube and Burnett (1997b, 2000), Straube (1998)	[113,144-147]
Denmark	Jessing (1959), Korsgaard and Madsen (1962a, 1962b, 1964a, 1964b)	[148,126-129]
France	Flori (1990, 1991, 1992)	[149-151]
Germany	Künzel (1976, 1993), Künzel and Schwarz (1968), Schwarz (1973b), Frank et al. (1977)	[152-156]
Norway	Holmgren (1946), Holmgren et al. (1949), Hoppestad (1951, 1955), Svendsen (1955), Isaksen (1965, 1975)	[121-125,157, 158]
Portugal	Henriques (1992)	[159]
Singapore	Choi (1996, 1999a, 2001)	[130,131,132]
Sweden	Varnbo (1966), Järnmark (1968), Beijer (1976, 1977), Jacobson (1977)	[160-164]
United Kingdom	Beckett (1938), Lacy (1951b, 1958, 1964a, 1964b, 1965, 1977), Newman (1987), Brown (1988)	[66,110,119,120, 135-138,165]

* In this paper, no direct report of free WDR measurements is given but such measurements are reported to have been made at the Highett Laboratories of the Division of Building Research, CSIRO, Australia.

Table 2
Countries where field measurements of wind-driven rain on buildings have been/are being conducted (in alphabetical order)

Country	Author(s) and date of publication	References
Belgium	Meert and Van Ackere (1977, 1978), Ali Mohamed and Hens (1992), Hens and Ali Mohamed (1994), Bollen and Eerdekens (1998), Blocken and Carmeliet (2000a, 2000b, 2002), Blocken et al. (2001).	[143,168-175]
Canada	Ritchie and Davison (1969), Straube et al. (1995), Straube and Burnett (1997a, 1997b, 2000), Straube (1998)	[112,113,144-147]
Denmark	Korsgaard and Madsen (1964a, 1964b), Kragh (1998)	[128,129,176]
France	Croiset (1957), Hilaire and Savina (1988), Flori (1990, 1991, 1992)	[133,149-151,177]
Germany	Künzel and Schwartz (1968), Künzel (1970, 1986, 1993), Künzel et al. (1971), Helbig (1972), Schwarz (1973a, 1973b), Frank (1973), Scultetus (1974), Lammel and Metzig (1997), Kerr and Freathy (1998)	[153-155,178-186]
Japan	Ishizaki et al. (1970), Ito et al. (1983), Ishikawa (1988)	[187-189]
Netherlands	Basart (1946), van Mook (1996, 1998a, 1998b, 1999a, 1999b, 2002), Högberg et al. (1999)	[104-106,166, 190-193]
Norway	Isaksen (1965), Isaksen (1975)	[157,158]
Portugal	Henriques (1992)	[159]
Sweden	Ryd (1970), Holmgren (1972), Sandin (1973, 1980, 1984, 1987, 1991, 1994), Beijer (1976, 1977), Jacobson (1977), Lyberg (1979, 1980), Högberg (1998, 1999a, 1999b, 2002), Adl-Zarrabi and Högberg (2001)	[109,162-164,194-207]
United Kingdom	Lacy (1959, 1964a, 1964b, 1965, 1977), Hendry (1964), Harrison and Bonshor (1970), Cronshaw (1971), Herbert (1974), Whiteside et al. (1980), Newman (1987), Prior and Newman (1988), Brown (1988), Osmond (1995, 1996), Kerr et al. (1997), Kerr and Freathy (1998)	[66,68,110, 136-138,165, 167,186,208-215]
USSR (former)	Tsvid (1960)	[216]

Table 3
Countries for which wind-driven rain maps have been prepared (in chronological order)

Country	Author(s) and date of publication	References
Norway	Hoppestad (1955)	[124]
Denmark	Jessing (1959, 1966)	[148,228]
United Kingdom/Ireland	Lacy and Shellard (1962), Lacy (1965, 1971, 1976, 1977)	[66,138,226, 227,234]
Canada	Boyd (1963)	[240]
Poland	Blociszewski (1966)	[229]
Rumania	Jonesen and Marcu (1966)	[230]
Spain	Avendano (1966)	[231]
Sweden	Varnbo (1966), Järnmark (1968)	[160,161]
former Western Germany	Caspar (1966)	[232]
former USSR (European part)	Shver (1971)	[241]
former Eastern Germany	Eichler (1970a, 1970b)	[242,243]
USA	Grimm (1982), Underwood and Meentemeyer (1998)	[244,245]
China	Sauer (1987)	[246]
India	Chand and Bhargava (2002)	[247]

Table 4
Obstruction factor as a function of the distance of the obstruction from the wall, as provided by the European Standard Draft (CEN 1997, [238])

Distance of obstruction from wall (m)	Obstruction factor O
4 - 8	0.2
8 - 15	0.3
15 - 25	0.4
25 - 40	0.5
40 - 60	0.6
60 - 80	0.7
80 - 100	0.8
100 - 120	0.9
> 120	1.0

Table 5
Results of the numerical simulation of wind-driven rain as obtained by Choi [96]. Catch ratios are given for each of the 12 areas on the windward facade of the building, for different wind speed and different horizontal rainfall intensity. Wind direction is perpendicular to the facade.

Catch ratios for various horizontal rainfall intensities									
	Wind speed 10 m/s			Wind speed 20 m/s			Wind speed 30 m/s		
R_h (mm/h)	10	30	50	10	30	50	10	30	50
S4	0.46	0.47	0.47	1.19	1.18	1.17	2.37	2.21	2.15
S3	0.19	0.22	0.23	0.87	0.86	0.86	1.90	1.80	1.76
S2	0.13	0.15	0.16	0.72	0.73	0.73	1.69	1.62	1.60
S1	0.09	0.11	0.11	0.47	0.50	0.51	1.43	1.40	1.39
C4	0.41	0.43	0.44	1.23	1.18	1.16	2.20	2.08	2.03
C3	0.14	0.18	0.19	0.74	0.77	0.77	1.78	1.70	1.67
C2	0.08	0.11	0.12	0.61	0.64	0.65	1.58	1.53	1.51
C1	0.05	0.07	0.08	0.34	0.40	0.43	1.31	1.30	1.30

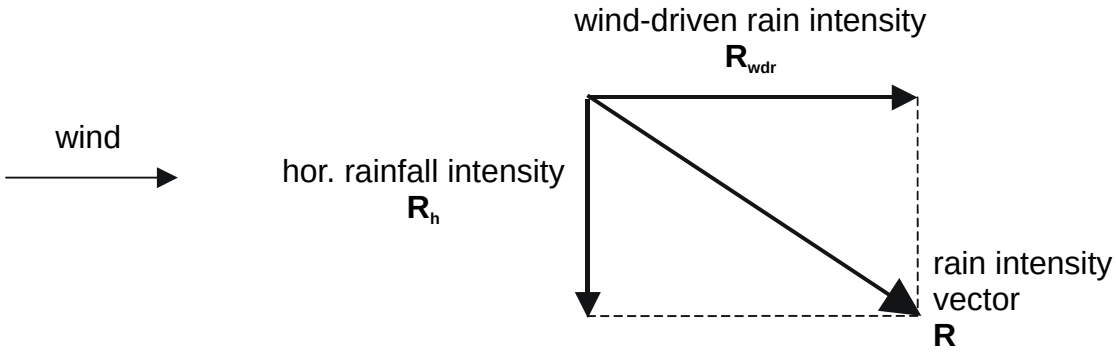
wind-driven rain intensity
R_{wdr}
wind
hor. rainfall intensity
R_h
rain intensity
vector
R

FIGURE 1

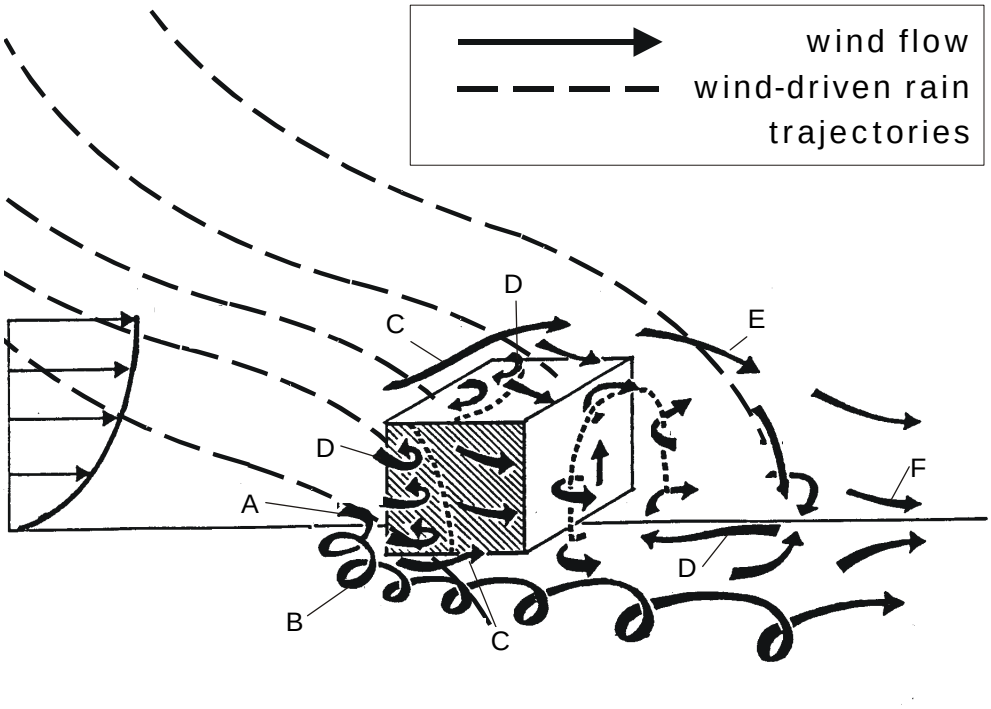

FIGURE 2

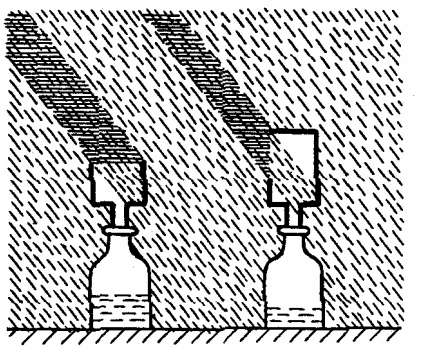

FIGURE 3

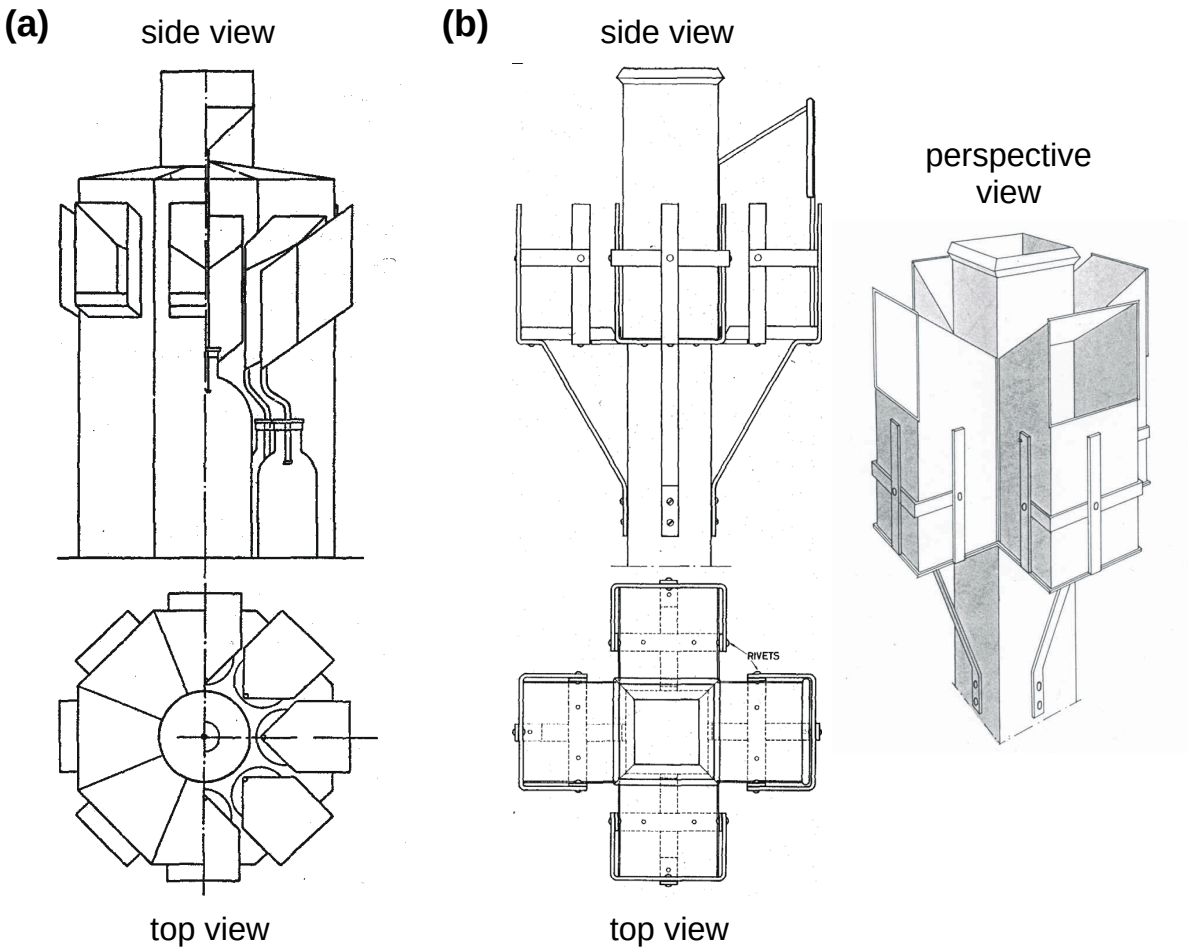
(a)
side view
top view
(b)
side view
RIVETS
top view
perspective
view

FIGURE 4

(a)

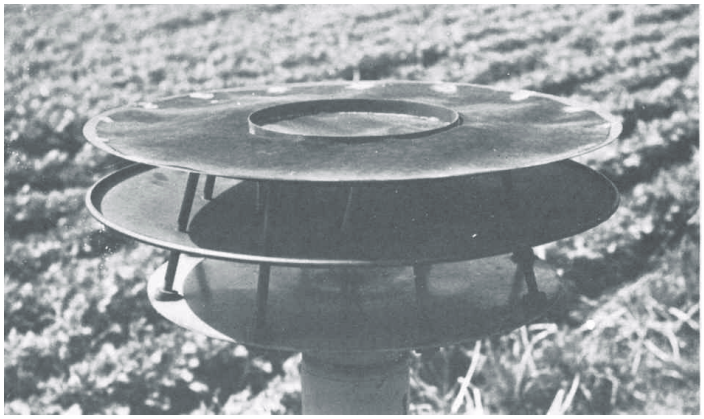

(b)

FIGURE 5

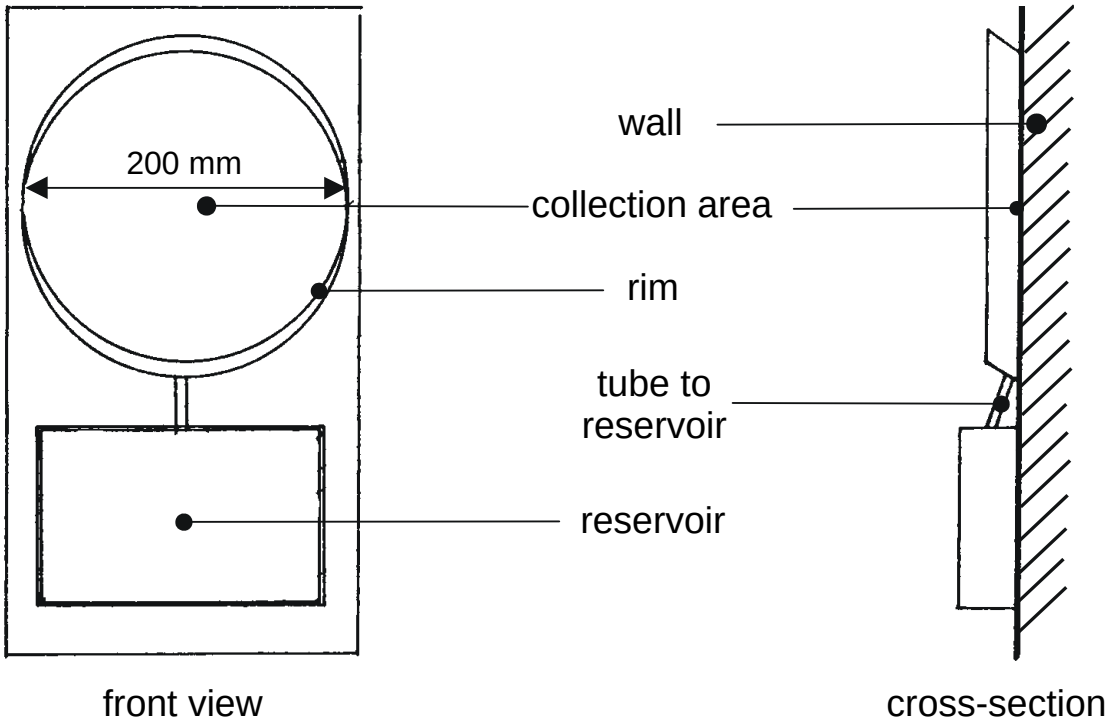
200 mm
wall
collection area
rim
tube to
reservoir
reservoir
front view
cross-section

FIGURE 6

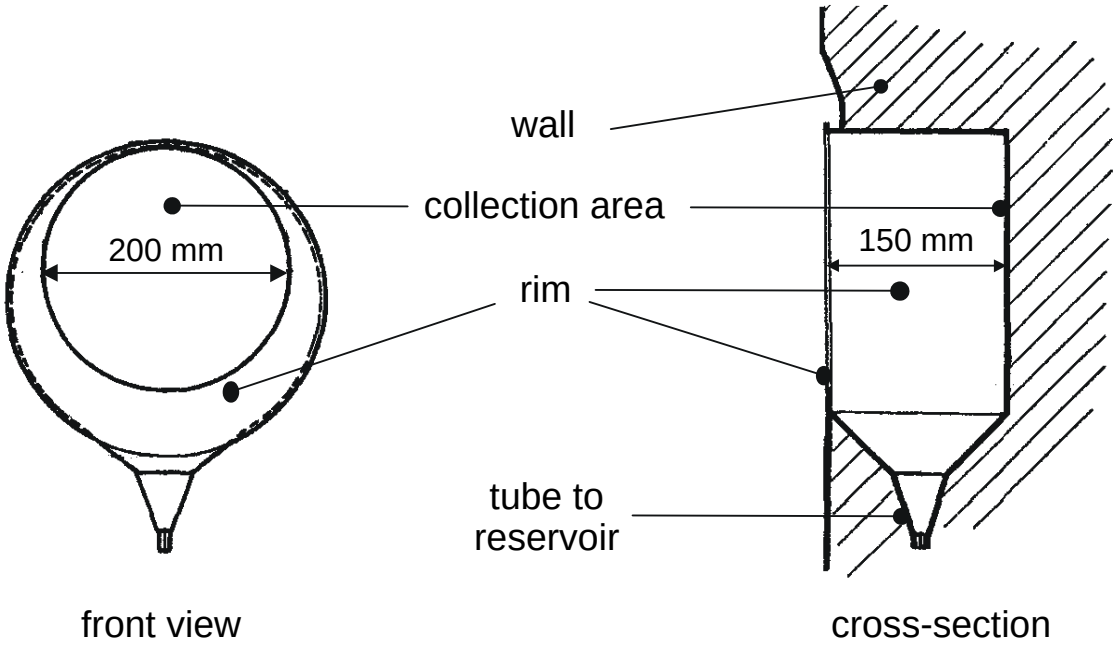
wall
collection area
200 mm
150 mm
rim
tube to
reservoir
front view
cross-section

FIGURE 7

(a)

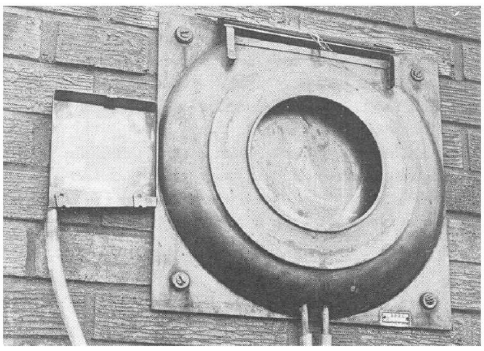

(b)

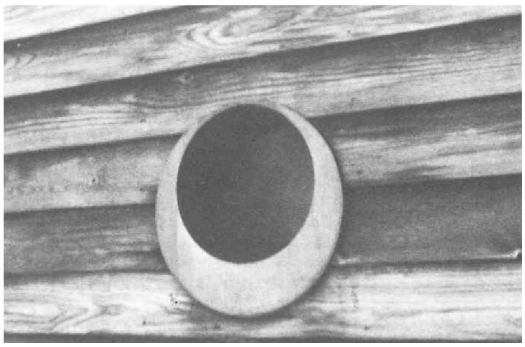

FIGURE 8

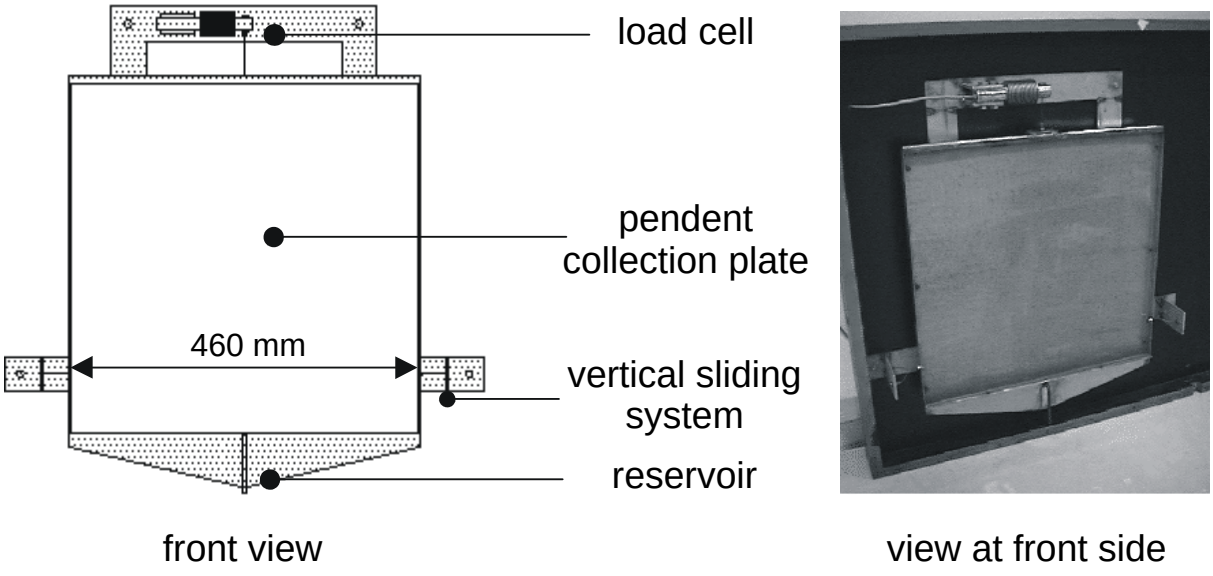
load cell
pendent
collection plate
460 mm
vertical sliding
system
reservoir
front view
view at front side

FIGURE 9

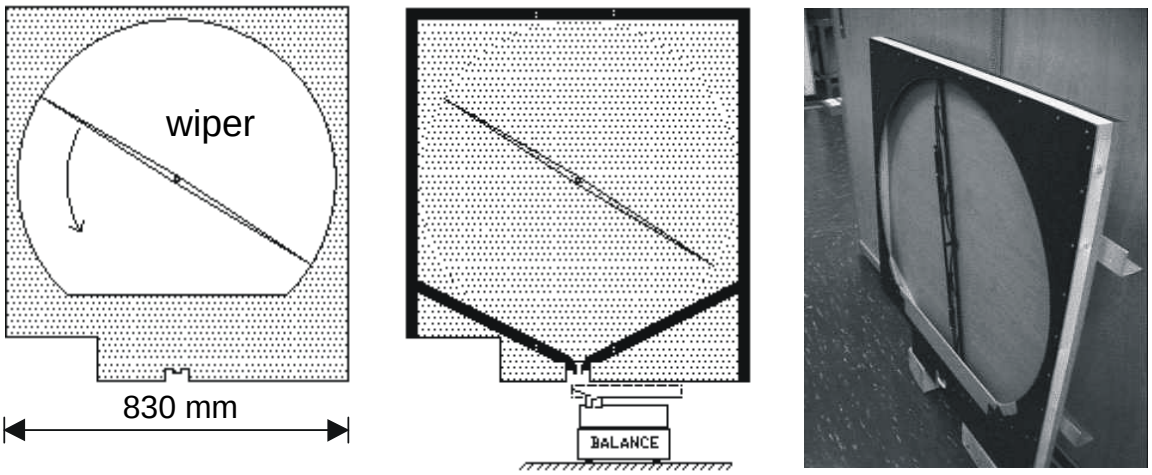

front view | rear view (back plate removed) | view at front side

FIGURE 10

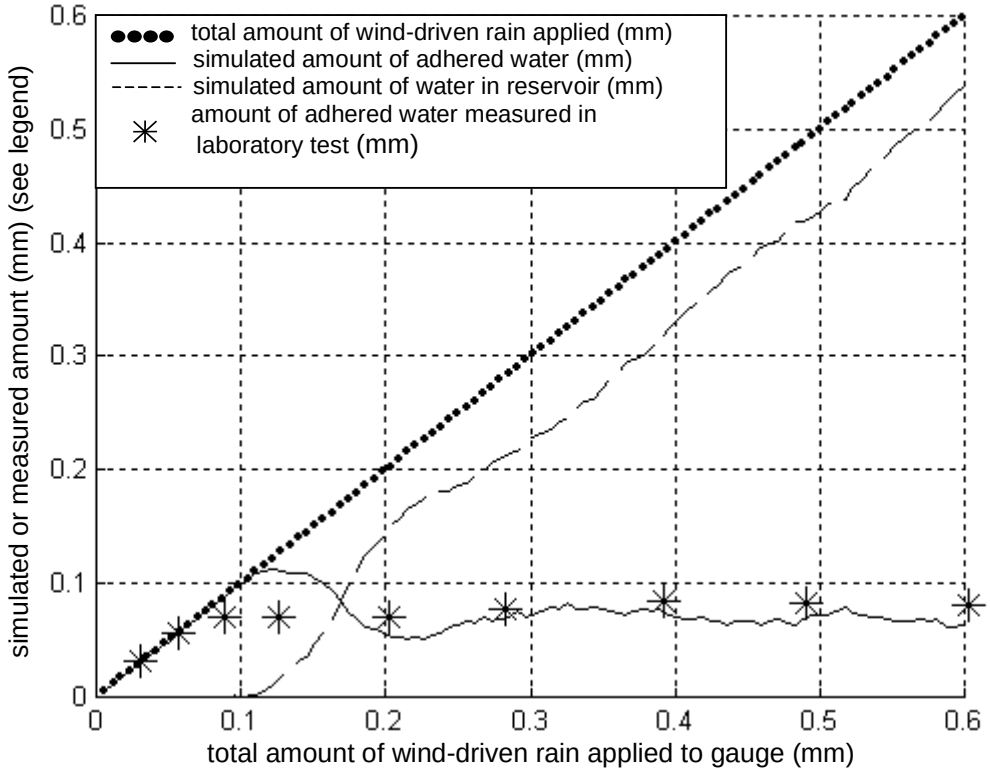
total amount of wind-driven rain applied (mm)
simulated amount of adhered water (mm)
simulated amount of water in reservoir (mm)
amount of adhered water measured in laboratory test (mm)
simulated or measured amount (mm) (see legend)
total amount of wind-driven rain applied to gauge (mm)
0
0.1
0.2
0.3
0.4
0.5
0.6

FIGURE 11

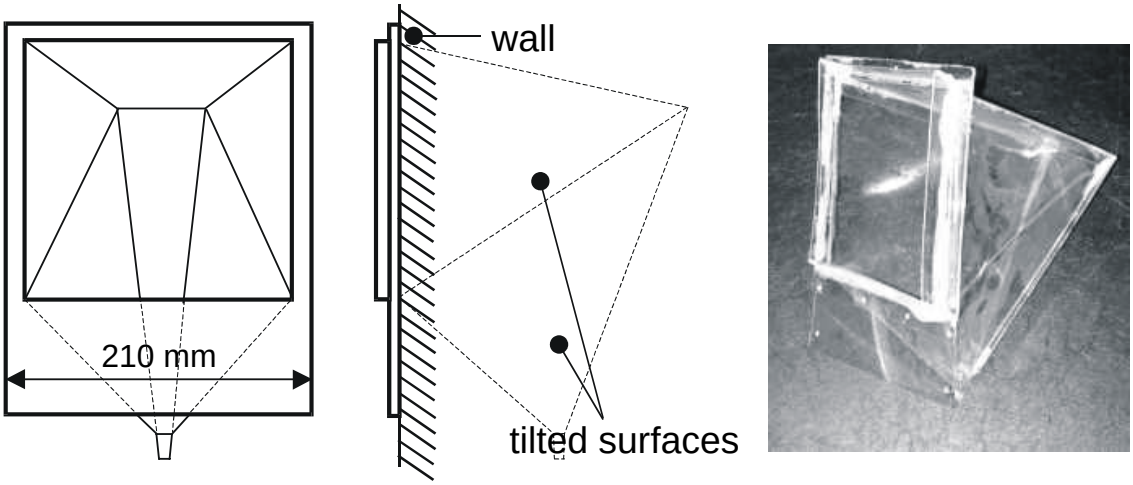

front view side view perspective view

FIGURE 12

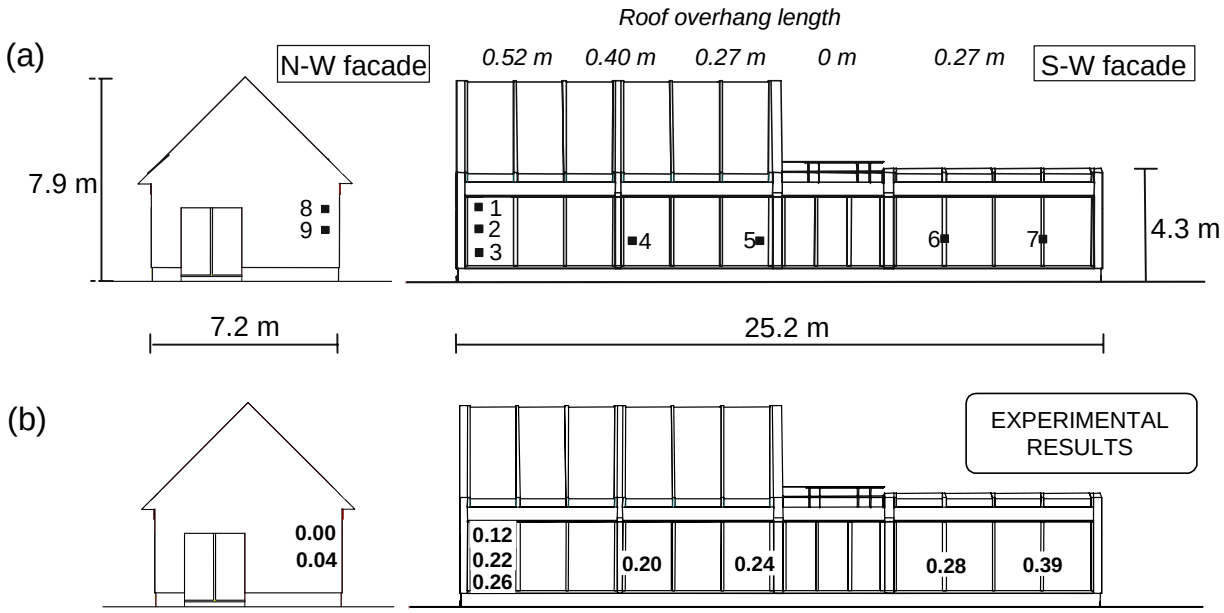
(a)
N-W facade
Roof overhang length
0.52 m
0.40 m
0.27 m
0 m
0.27 m
S-W facade
7.9 m
8
9
1
2
3
4
5
6
7
4.3 m
7.2 m
25.2 m
(b)
EXPERIMENTAL RESULTS
0.00
0.04
0.12
0.22
0.26
0.20
0.24
0.28
0.39

FIGURE 13

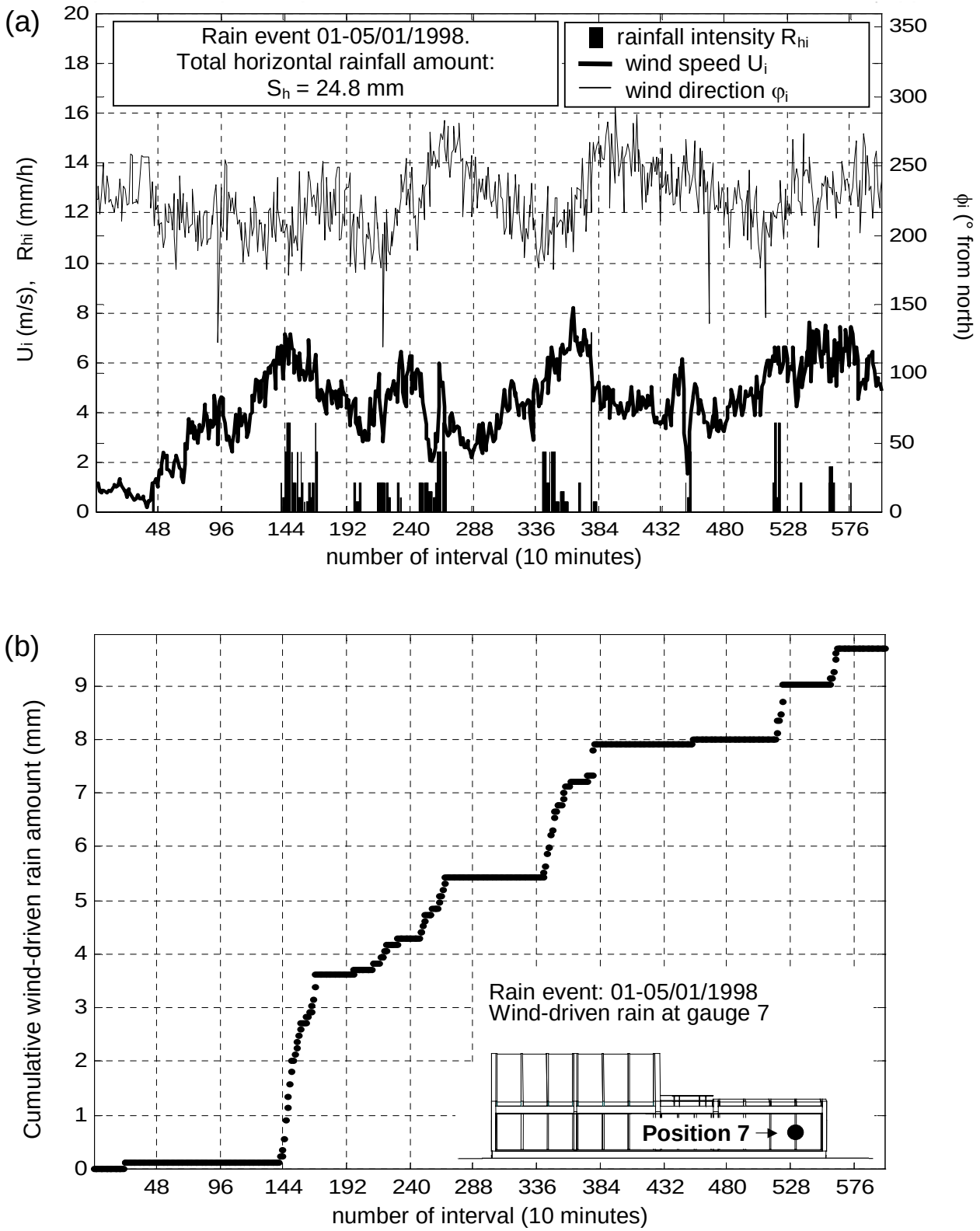
(a)
Rain event 01-05/01/1998.
Total horizontal rainfall amount:
S_h = 24.8 mm
rainfall intensity R_{hi}
wind speed U_i
wind direction φ_i
U_i (m/s), R_{hi} (mm/h)
φ_i (° from north)
number of interval (10 minutes)
(b)
Cumulative wind-driven rain amount (mm)
Rain event: 01-05/01/1998
Wind-driven rain at gauge 7
Position 7
number of interval (10 minutes)

FIGURE 14

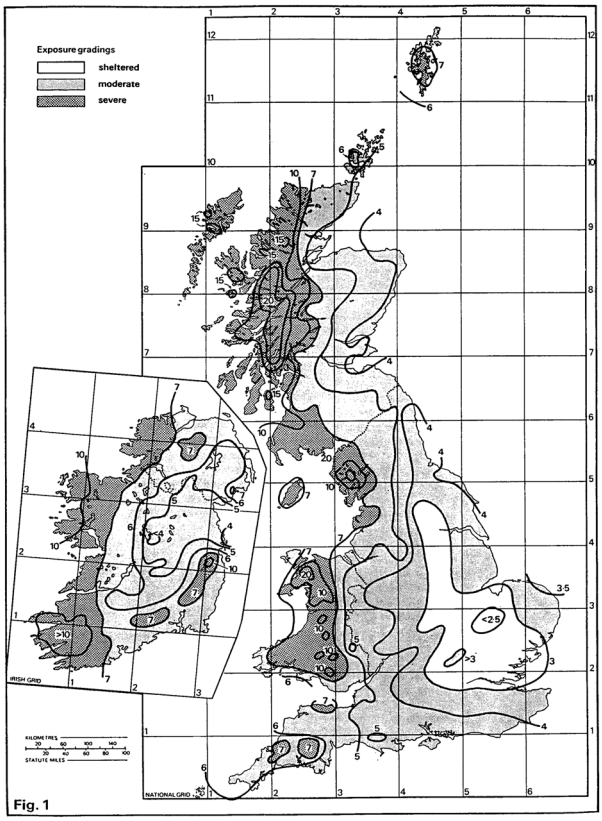

Fig. 1

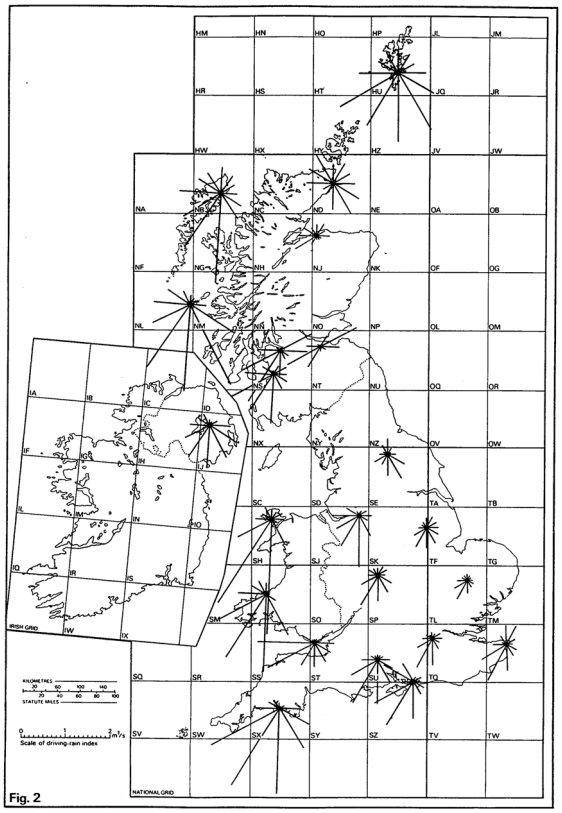

Fig. 2

FIGURE 15

Description of wall	Average value	Distribution
Two storey gable	0.4	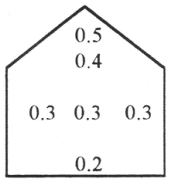
Three storey gable	0.3	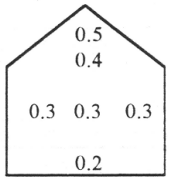
Multi storey flat roof[1]	0.2 for e.g. ten storey, but higher intensity at top	0.5 for top 2.5 m 0.2 for remainder
two storey eaves wall	0.3	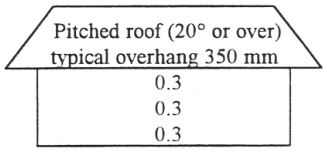
three storey eaves wall	0.4	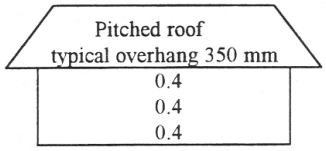
two storey flat roof (pitch <20°)	0.4	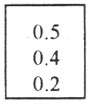
1) These data apply to multi-storey blocks of normal aspect width; no data are available for exceptionally narrow buildings		

FIGURE 16

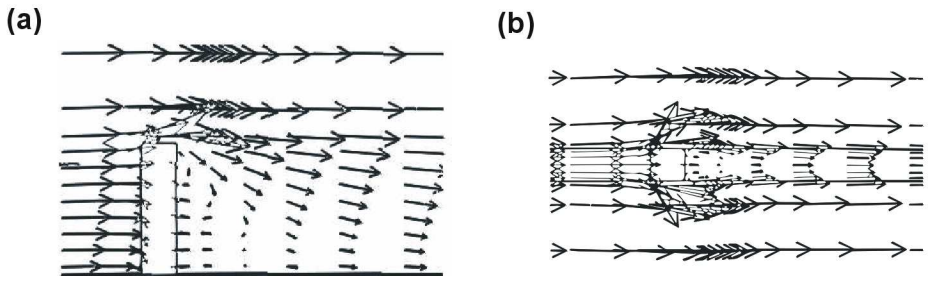

FIGURE 17

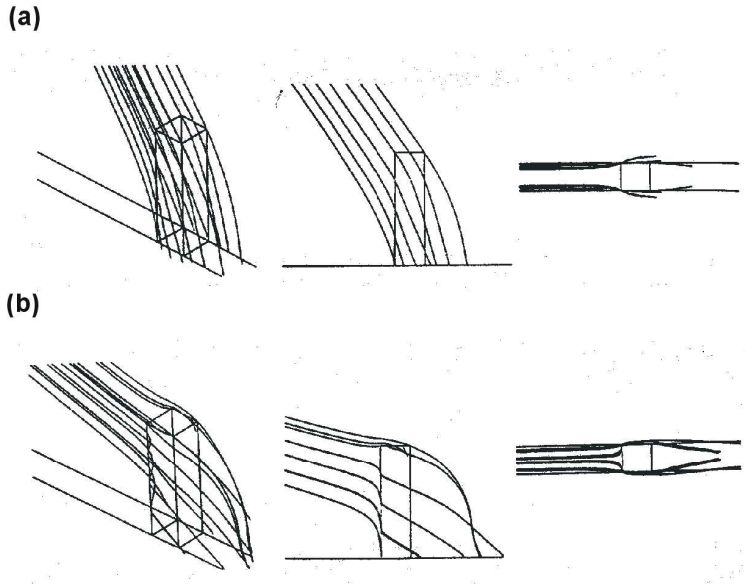

FIGURE 18

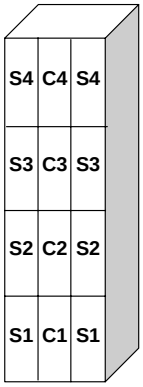

FIGURE 19

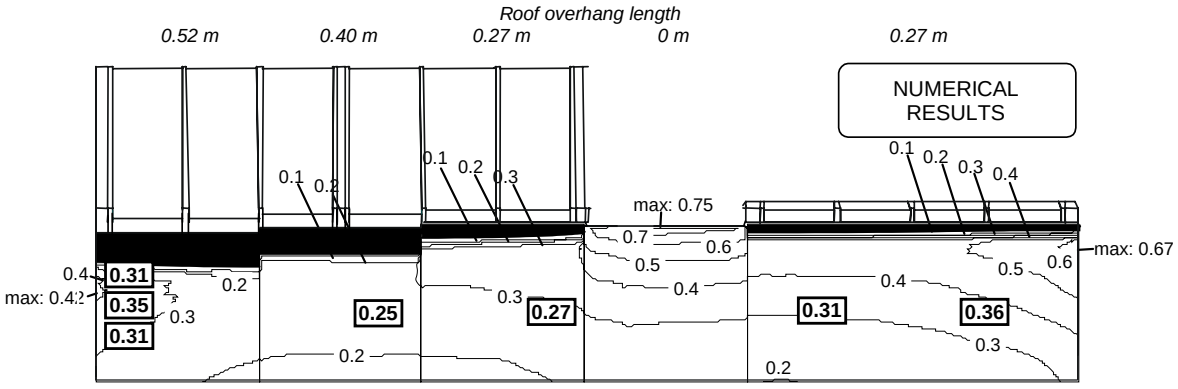
Roof overhang length
0.52 m
0.40 m
0.27 m
0 m
0.27 m
NUMERICAL RESULTS
0.1
0.2
0.3
0.4
max: 0.75
0.7
0.6
0.5
0.4
max: 0.67
0.6
0.5
0.4
0.3
0.2
0.1
0.2
0.1
0.2
0.3
0.4
0.31
0.35
0.31
0.3
0.25
0.27
0.31
0.36
0.3
0.2
0.2

FIGURE 20

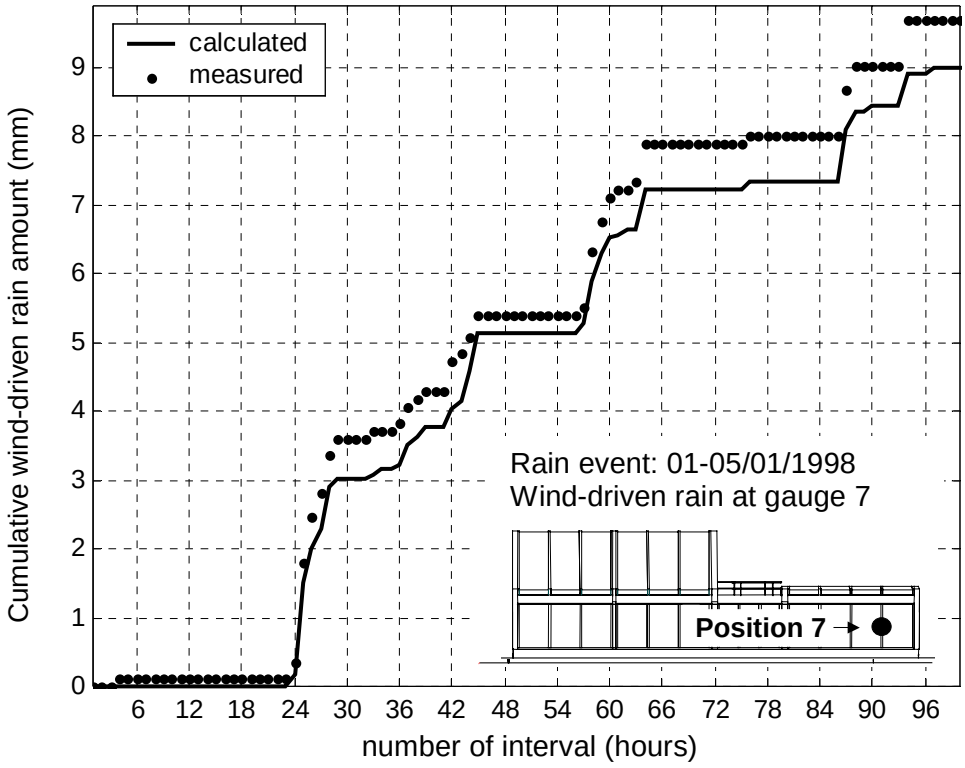
calculated
measured
Cumulative wind-driven rain amount (mm)
number of interval (hours)
Rain event: 01-05/01/1998
Wind-driven rain at gauge 7
Position 7
0
1
2
3
4
5
6
7
8
9
6
12
18
24
30
36
42
48
54
60
66
72
78
84
90
96

FIGURE 21